

Evolution of a chemically reacting plume in a ventilated room

By **D. T. CONROY, STEFAN G. LLEWELLYN SMITH**
AND **C. P. CAULFIELD**

Department of Mechanical and Aerospace Engineering, Jacobs School of Engineering,
UCSD, 9500 Gilman Drive, La Jolla, CA 92093-0411, USA

(Received 4 November 2004 and in revised form 22 February 2005)

The dynamics of a second-order chemical reaction in an enclosed space driven by the mixing produced by a turbulent buoyant plume are studied theoretically, numerically and experimentally. An isolated turbulent buoyant plume source is located in an enclosure with a single external opening. Both the source and the opening are located at the bottom of the enclosure. The enclosure is filled with a fluid of a given density with a fixed initial concentration of a chemical. The source supplies a constant volume flux of fluid of different density containing a different chemical of known and constant concentration. These two chemicals undergo a second-order non-reversible reaction, leading to the creation of a third product chemical. For simplicity, we restrict attention to the situation where the reaction process does not affect the density of the fluids involved. Because of the natural constraint of volume conservation, fluid from the enclosure is continually vented. We study the evolution of the various chemical species as they are advected by the developing ventilated filling box process within the room that is driven by the plume dynamics. In particular, we study both the mean and vertical distributions of the chemical species as a function of time within the room. We compare the results of analogue laboratory experiments with theoretical predictions derived from reduced numerical models, and find excellent agreement. Important parameters for the behaviour of the system are associated with the source volume flux and specific momentum flux relative to the source specific buoyancy flux, the ratio of the initial concentrations of the reacting chemical input in the plume and the reacting chemical in the enclosed space, the reaction rate of the chemicals and the aspect ratio of the room. Although the behaviour of the system depends on all these parameters in a non-trivial way, in general the concentration within the room of the chemical input at the isolated source passes through three distinct phases. Initially, as the source fluid flows into the room, the mean concentration of the input chemical increases due to the inflow, with some loss due to the reaction with the chemical initially within the room. After a finite time, the layer of fluid contaminated by the inflow reaches the opening to the exterior at the base of the room. During an ensuing intermediate phase, the rate of increase in the concentration of the input chemical then drops non-trivially, due to the extra sink for the input chemical of the outflow through the opening. During this intermediate stage, the concentration of the input chemical continues to rise, but at a rate that is reduced due to the reaction with the fluid in the room. Ultimately, all the fluid (and hence the chemical) that was originally within the room is lost, both through reaction and outflow through the opening, and the room approaches its final steady state, being filled completely with source fluid.

1. Introduction

In many industrial settings, pipelines transport pressurized chemicals in the liquid state that would undergo a chemical reaction if exposed to air. If a leak were to occur, the chemical would enter the ambient environment, and under ambient pressure, vaporize and cool, forming a gas, with in general a different density from the ambient air. Provided the source remains relatively isolated, and the leaking fluid has some initial momentum, which is a plausible scenario, the resulting plume, driven by buoyancy, would inevitably entrain ambient air. This entrainment would have two principal effects. First, it would increase the volume of air that is at least partially contaminated by the released chemical. Secondly, it would allow the released chemical to react with the entrained air. This air, contaminated with both the original chemical and the reaction product, would thus start to fill the space. From a hazard analysis viewpoint, it is clearly important to understand the spatial and temporal evolution of this contamination. For example, such an understanding would allow the identification of the time available to evacuate a building before concentrations of either the released chemical or the product became hazardous. Naturally, similar concerns also arise when the release of the hazardous reacting chemical is intentional, and many of the scientific and theoretical modelling issues are the same.

Furthermore, situations with analogous physical properties occur in geophysics. For example, in oceanography, a few decades ago deep-sea hydrothermal vents (known as 'black smokers' because they discharge a black precipitate composed of sulphur-bearing material) were discovered at mid-ocean ridges. Hot seawater and sulphites, formed in hot magma chambers below the surface, seep out of the ground as a low-density fluid. Although there are significant thermal differences between the vented fluid and the surrounding ambient seawater, there is no vaporization because of the high pressure. The vented buoyant fluid forms a turbulent plume that when mixed with the cold ambient seawater creates a precipitate that can be seen as black smoke. Since these regions are far underwater and essentially devoid of sunlight, new organisms have been found to thrive on the chemically rich seawater using chemosynthesis as an energy source. These regions support a unique ecosystem critically dependent on the concentrations of the chemicals issuing from the plumes, which is of great interest to researchers in biology and oceanography (Tunnicliffe 1992). Due to the local topography, and also to the ambient stratification of the ocean (see Cardoso & Woods 1993), the plume fluid propagates only a finite distance away from the source, and so there are marked points of similarity with the industrial situation.

The fundamental fluid dynamical aspect of this class of problems is the presence within a finite, though large, restricted area, or 'room' (with limited 'ventilation' to the exterior) of an isolated source of fluid of both different density and different chemical composition from the fluid initially within the room. In the absence of chemical reaction between the source and ambient fluid, such flows have been widely studied, building upon the original seminal contribution of Baines & Turner (1969, henceforth BT69). They considered the flow that develops when an isolated source of buoyancy alone (a so-called 'point source plume') issues into an enclosed region. As the plume rises it entrains ambient fluid (in a way that is well modelled by the classic approach of Morton, Taylor & Turner 1956, henceforth MTT56), until ultimately the plume fluid reaches the ceiling of the room, where, provided the aspect ratio of the room is sufficiently small, it spreads out, and forms a 'first front' of fluid that has been cycled through the plume. As the plume continues to entrain, the first front moves downward through the room, and the region above the first front fills with fluid that has, at

some stage, been entrained into the plume. This filling box mechanism continues for all times if the source has zero volume flux, as the first front only approaches the source height asymptotically.

The evolution of the density distribution within the room can be accurately studied numerically using the numerical algorithm initially proposed by Germeles (1975). Essentially, this algorithm makes a quasi-steady approximation, assuming that the transit time of a fluid parcel within the plume from floor to ceiling is very much faster than the transit time for a fluid parcel within the room from the ceiling to the floor. This assumption is satisfied provided the source is isolated and always occupies a negligibly small fraction of the cross-sectional area of the room at all heights, and so the aspect ratio of the room is sufficiently small. In such a circumstance, the evolution of the plume can be considered to occur in a quiescent ambient. At any time instant, once the properties (and in particular the volume flux) of the plume are determined at all heights, the evolution of the ambient density distribution in the room can be determined by tracking the motion of a sufficiently large number of layers of ambient fluid. The propagation of each of the interfaces between the layers is determined by requiring that the upflow volume flux in the plume at that height is balanced by a slower downflow of ambient fluid, with the effect that entrainment into the plume causes neighbouring interfaces to move closer together. This method, discussed in more detail below, leads to an accurate representation of the evolution of the ambient density distribution within the room.

A particularly important aspect of the point source model that deserves attention is the requirement that the source has finite buoyancy flux yet zero volume flux. This corresponds formally to the requirement that there is no lower bound on the fluid density within the system. Therefore, the density of the layer above the first front continues to decrease without limit, with an asymptotic vertical structure in the density profile, consistent with the assumption that the buoyancy flux in the plume varies linearly with distance from the source (see Worster & Huppert 1983).

Caulfield & Woods (2002, henceforth CW02) generalized this flow to consider the behaviour when the source has a non-zero source volume flux. This source volume flux changes the behaviour of the system qualitatively in several ways. First, since the source has a constant finite volume flux (and for consistency also a finite source momentum flux), there is a minimum fluid density within the system, corresponding to the density of the fluid issuing from the source. In the limit of long time, the fluid in the room approaches this density asymptotically. Secondly, since there is a finite volume flux into the system, there must be at least one opening to the exterior, or vent, to allow for conservation of volume. Furthermore, the first front arrives at the location of the opening in finite time, and for the particularly straightforward case where the source and the opening are both at the floor of the room, this implies that the entire room becomes filled in a finite time with fluid that has been cycled through the plume, and contaminated fluid starts to issue from the opening. Since the fluid in the vicinity of the source becomes less dense than the initial ambient fluid, if the source volume flux is constant, the source buoyancy flux decreases. Therefore, as discussed in CW02 in detail, the source starts to behave less and less like a buoyant plume, and more and more like a forced jet. Indeed, asymptotically, as the fluid throughout the room approaches the density of the source fluid, the source ceases to be buoyant, and the flow within the room is driven by a source of momentum alone, enabling the development of an asymptotic analytical model for the evolution of the density

within the room which is a (slight) improvement on that discussed by Worster & Huppert (1983) and BT69.

None of these studies however considered the possibility of chemical reaction between the source fluid and ambient fluid within the room, and so in this paper we generalize the previous work to consider the behaviour of a system where the source fluid and the fluid initially within the room chemically react. For there to be a possibility of chemical reaction, it is clearly necessary for there to be a finite volume flux of source fluid into the enclosed space, and so there must be at least one vent to conserve fluid volume. As a first attempt to consider this class of problems, we will restrict ourself to flows with vents at a single height, thus avoiding the possibility of the development of different steady states, as can occur when there are two vents at different heights (see Woods, Caulfield & Phillips 2003). Generalizing CW02, we therefore restrict our attention to the simplest case, where the source and a single external opening are at the same location, the floor of the room. Of course, the same model can apply to flows with multiple openings at the same height, provided unidirectional flow occurs through each opening. Furthermore, to gain an understanding of the extent to which the filling box flow itself affects the evolution of the chemically reacting species, we assume that the reaction has no effect on the flow dynamics, i.e. as the different species react they have no effect on the fluid density, and so play a passive role on the flow dynamics. This problem still exhibits a rich range of flow behaviours, and has the particular attractions that it is a simple generalization of previous studies and that the results of theoretical predictions can be tested experimentally.

The paper is therefore organized as follows. In §2, we briefly review the standard plume model due to MTT56, and discuss the generalizations required to model flow within an enclosed space (as discussed in BT69) with a finite volume flux and a single vent (CW02). We add to this model the evolution of passively advected reactive species, one initially in the plume source and the other initially in the enclosed space. We also generate simplified well-mixed models which ignore the plume dynamics, and the associated vertical distribution induced by the plume within the room. Once we have developed these models and identified the critical governing parameters and the important time scales for the flow, in §3, we present the results of time-dependent numerical solutions of this model for various relevant choices of the parameters. We discuss in some detail the inherent assumptions of the model, which place some restrictions on the possible choices of the various flow parameters. In §3, the solution is generated using the method originally proposed by Germeles (1975) appropriately modified to track the dynamically passive concentrations of the various chemical species both within the plume and in the interior of the room. In §4, we discuss the experimental method which we have used to consider the flow under consideration, in particular the chemicals which we have identified to have the appropriate properties. We then compare the results of the experiments with the various theories and numerical models which we have developed to investigate their usefulness, identifying points of agreement and discussing reasons for observed discrepancies. Finally, in §5, we draw some conclusions.

2. Model description

There are three components to the required model: a model for the isolated plume source; a model for the induced flow within the room; and a model for the chemical reactions between the different species. We consider each in turn. The flow geometry and the notation used is shown in figure 1.

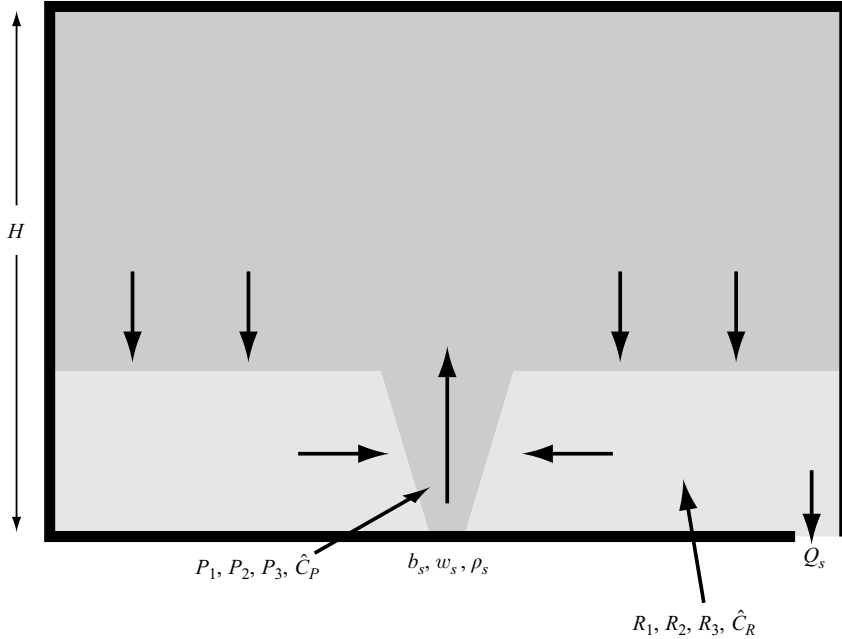


FIGURE 1. Schematic representation of the flow geometry. A turbulent plume source is located at $z=0$ in a room of depth H with a single external opening also at $z=0$. The plume has fixed source radius b_s , source velocity w_s and source density ρ_s , so that the source density concentration $\hat{C}_P(0, t) = 1$ as defined in (2.21). The source fluid also has fixed concentration P_{10} of species one alone. The room is initially filled with fluid of density $\rho_{R0} > \rho_s$, corresponding to room density concentration $\hat{C}_R(z, 0) = 0$ as defined in (2.21) and concentration R_{20} of species two alone. As the plume rises and entrains fluid, the plume fluid has concentrations $P_1(z, t)$, $P_2(z, t)$, $P_3(z, t)$ and $\hat{C}_P(z, t)$ of the reacting species one and two, the product species three, and the fluid density respectively. Similarly, as the filling box process modifies the stratification in the room, the room fluid has concentrations $R_1(z, t)$, $R_2(z, t)$, $R_3(z, t)$ and $\hat{C}_R(z, t)$ of the reacting species one and two, the product species three, and the fluid density respectively. Eventually, due to the continual venting (with flux Q_s) of room fluid through the external opening, $R_1 \rightarrow P_{10}$, $\hat{C}_R \rightarrow 1$, $R_2, R_3 \rightarrow 0$, as the room becomes completely filled with source fluid. When we consider well-mixed models, we ignore any distinction between plume fluid and room fluid, and consider well-mixed concentrations W_1, W_2 and W_3 of the three chemical species and concentration \hat{C}_W of the fluid density.

2.1. Plume dynamics

We consider an isolated source of fluid of finite extent, supplying fluid of different density and velocity compared to the surrounding environment. We make the Boussinesq assumption, and so suppose that the density differences involved are sufficiently small so that they only affect the buoyancy force. Although the dynamics of the ensuing plume are highly turbulent and irregular at sufficiently high Reynolds number, MTT56 demonstrated that the dynamics of the evolving plume can be understood well through consideration of the behaviour of three integrated conserved quantities: the volume flux πQ , the specific momentum flux πM and the specific buoyancy flux πB , defined as

$$\pi Q(z, t) = \frac{2\pi}{T_t} \int_{t-T_t/2}^{t+T_t/2} \int_0^\infty r w_p dt dr = \pi \bar{w}_p b^2, \tag{2.1a}$$

$$\pi M(z, t) = \frac{2\pi}{T_t} \int_{t-T_t/2}^{t+T_t/2} \int_0^\infty r w_p^2 dt dr = \pi \bar{w}_p^2 b^2, \quad (2.1b)$$

$$\begin{aligned} \pi B(z, t) &= \frac{2\pi}{T_t} \int_{t-T_t/2}^{t+T_t/2} \int_0^\infty r w_p g \frac{\rho_R - \rho_P}{\rho_{R0}} dt dr \\ &= \pi g \frac{\rho_R - \bar{\rho}_P}{\rho_{R0}} \bar{w}_p b^2 = \pi g'_P \bar{w}_p b^2. \end{aligned} \quad (2.1c)$$

In the equations above $w_p(r, z, t)$ and $\rho_P(r, z, t)$ are the vertical velocity and density profiles in the plume, ρ_R is the ambient density, ρ_{R0} is a reference density, the initial (constant) density in the room, and g'_P is the reduced gravity of the plume relative to the local ambient fluid. Bars denote averages over the plume. The various fluxes are in general time-dependent, but we take a rolling time average to smooth out turbulent fluctuations over time scales substantially shorter than a characteristic time scale T_t . For simplicity we assume that the flow in the plume has a top hat profile, i.e. the vertical velocity and density take one value inside the plume and another value outside: at all heights and times the plume is defined with a characteristic radius $b(z, t)$. (This makes it clear that consideration of the three fluxes Q , M and B is equivalent to consideration of the three characteristic properties of the plume: its radius b , its velocity w_p and the plume reduced gravity g'_P .) As discussed in MTT56, it is straightforward to derive governing equations for the fluxes within a plume under the assumption that the characteristic entrainment velocity u_e can be related to the vertical velocity w_p at every height within the plume by a universal constant of proportionality, the so-called entrainment constant α , to yield

$$\frac{\partial Q}{\partial z} = 2\alpha M^{1/2}, \quad (2.2a)$$

$$\frac{\partial M}{\partial z} = \frac{BQ}{M}, \quad (2.2b)$$

$$\frac{\partial B}{\partial z} = \frac{g}{\rho_{R0}} \frac{\partial \rho_R}{\partial z} Q = -N^2 Q, \quad (2.2c)$$

where N^2 is the buoyancy frequency.

2.2. Room dynamics

The equations discussed above are closed provided source conditions Q_s , M_s and B_0 for volume flux, momentum flux and initial buoyancy flux (or equivalently source radius, velocity and density) are given, and there is some mechanism to determine the ambient density distribution outside the plume. In the circumstance we are considering, namely that of an isolated single plume rising from the bottom ($z = 0$) of an enclosed space with one vent at the same level as the source, the ambient density is coupled to, and determined by, the plume dynamics in a straightforward manner, as discussed in more detail in CW02. We assume that the plume is sufficiently isolated (i.e. $b^2 \ll A_c$ at all heights in the room, where A_c is the cross-sectional area of the room) for the entrainment into the plume to be essentially horizontal. Therefore, the fluxes evolve as the plume rises in the room in a manner that is well approximated by equations (2.2).

However, when the plume reaches the ceiling, the upper boundary forces the fluid at the top of the plume to spread out horizontally like a gravity current. As discussed in BT69 and considered in more detail in Hunt, Cooper & Linden (2001) provided the aspect ratio and the source momentum flux are sufficiently small, a

filling box flow then develops, and the fluid from the gravity current descends in well-organized horizontal layers into the room, surrounding the plume when it encounters the sidewalls. Therefore, the ambient density distribution evolves in a time- and depth-dependent manner due to the continual arrival of plume fluid at the ceiling.

This evolving ambient density also affects the plume behaviour through entrainment. Indeed, as fluid is entrained into the plume there must be a return flow in the room to conserve mass. BT69 demonstrated that for a confined room if the plume occupies a negligible cross-sectional area (and so $\pi b^2 \ll A_c$ as already assumed) of the room then the return flow is uniform and given by the volume conservation relation

$$w_R A_c \simeq -\pi Q, \quad (2.3)$$

where w_R is the vertical velocity of the ambient fluid in the room. Assuming that the flow is sufficiently high Reynolds number so that the effects of diffusion can be ignored compared to advection in the equation for conservation of mass for the fluid within the room, (2.3) can be used to obtain

$$\frac{\partial \rho_R}{\partial t} = \frac{\pi Q}{A_c} \frac{\partial \rho_R}{\partial z}, \quad (2.4)$$

where we have used the fact that there is no net flow through the room owing to the vent and the source both being at the floor of the room. This equation closes the system given an initial density distribution of $\rho_R = \rho_{R0}$ within the room, leading to what is referred to as a ‘filling box process’.

It is important to appreciate that there is an essential quasi-steady approximation at the heart of the filling box process. Although the ambient density distribution in the room is evolving, it is assumed that it varies sufficiently slowly compared to the rising plume so that the plume can be assumed to be passing through a time-independent ambient density in the room. Equivalently to the assumption that the plume is isolated, the filling box process requires that the upward velocity w_p in the plume is always very much greater than the downward velocity in the environment, and so

$$\frac{M}{Q} \gg \frac{\pi Q}{A_c}. \quad (2.5)$$

Characteristic scaling for these quantities can be found by considering for simplicity the well-known ‘point source’ similarity solution, where the source is a source of buoyancy alone with $Q_s = 0 = M_s$. For this situation, the governing equations for flow in an unstratified environment admit a similarity solution

$$Q = \frac{6\alpha}{5} \left(\frac{9\alpha B_0}{10} \right)^{1/3} z^{5/3}, \quad M = \left(\frac{9\alpha B_0}{10} \right)^{2/3} z^{4/3}. \quad (2.6)$$

For this similarity solution, the plume velocity drops monotonically with distance from the source, while the volume flux naturally increases monotonically due to entrainment. Therefore, the most stringent restriction for (2.5) is at the ceiling, when $z = H$, in which case the validity condition becomes a condition on an aspect ratio parameter θ such that

$$\theta = \left(\frac{5}{6\alpha} \right)^2 \frac{A_c}{\pi H^2} \gg 1. \quad (2.7)$$

Therefore, we expect the quasi-steady approximation to be valid provided the aspect ratio of the room is sufficiently small, and hence the parameter θ is sufficiently large.

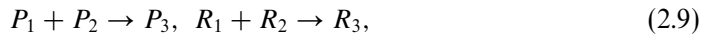
The source conditions (as noted on figure 1) that we choose to use are constant source radius b_s , source velocity w_s , and source density ρ_s , corresponding to constant source volume flux $Q_s = b_s^2 w_s$, source-specific momentum flux $M_s = b_s^2 w_s^2$, and initial source buoyancy flux $B_0 = g(\rho_{R0} - \rho_s)Q_s/\rho_{R0}$. As discussed in more detail in CW02, owing to the finite source volume flux and the location of the vent, the density of the ambient fluid at the source decreases below ρ_{R0} in finite time, as fluid that has been cycled through the plume reaches the external opening. Therefore, since $\rho_R(0) < \rho_{R0}$, if the source has a flux of constant-density fluid, the source buoyancy flux satisfies $B_s = g(\rho_R(0) - \rho_s)Q_s/\rho_{R0} < B_0$, and over time the source will behave less and less like the source of a buoyant plume, and more and more like the source of a forced momentum jet.

2.3. Chemistry dynamics

We now generalize the filling box process to allow for the time-dependent chemical reaction of different species. For simplicity, we do not allow the chemically reacting species to affect the flow dynamically. In particular, we assume that any heat of reaction is sufficiently small so that it does not affect the fluid density. This is a valid assumption for the experimental fluids and reactions which we consider in this paper. We consider the situation where two distinct species can react to form a third product species through a second-order reaction. Therefore, in general, we are interested in the spatial and temporal evolution of these three species both within the plume rising from the isolated source, and in the ambient fluid within the room. We denote the molar concentration of the three species within the plume as $P_1(z, t)$ and $P_2(z, t)$ for the reactants, and $P_3(z, t)$ for the product, while in the room we denote the equivalent quantities by $R_1(z, t)$, $R_2(z, t)$ and $R_3(z, t)$. The isolated plume source fluid is assumed to contain only species one with concentration P_{10} , while the room initially contains only species two, with concentration R_{20} . Therefore, the boundary and initial conditions are

$$P_2(0, t) = P_3(0, t) = R_1(z, 0) = R_3(z, 0) = 0, \quad P_1(0, t) = P_{10}, \quad R_2(z, 0) = R_{20}. \quad (2.8)$$

As ambient fluid is entrained into the plume in a height- and time-dependent manner, the concentration P_2 of species two within the plume fluid will increase from zero initially. Similarly, when the filling box process starts at the ceiling of the room, the concentration R_1 of species one at the ceiling will increase from zero. Once these dynamic effects have taken place, we then assume that a second-order non-reversible reaction takes place between the reacting species both in plume fluid rising from the isolated source and in the room. A second-order non-reversible reaction is a reaction of the form



in which the mutual presence of species one and two is necessary for the reaction and the reaction rate is proportional to the product of the concentrations of the two reacting species (for further details, see e.g. Levine 2002). Then

$$\frac{DP_1}{Dt} = \frac{DP_2}{Dt} = -K P_1 P_2, \quad \frac{DP_3}{Dt} = K P_1 P_2, \quad (2.10a)$$

$$\frac{DR_1}{Dt} = \frac{DR_2}{Dt} = -K R_1 R_2, \quad \frac{DR_3}{Dt} = K R_1 R_2. \quad (2.10b)$$

Here, the second-order rate constant $K(T, \mu)$ is determined experimentally for a particular reaction and may in general be a function of temperature T and, in the case of solutions, of ionic strength μ . D/Dt is the conventional convective derivative,

since the reaction is a Lagrangian process that advects passively with fluid parcels. The potential dependences on temperature and ionic strength are very important, because if the fluid density within the room is due to temperature or compositional differences (e.g. through varying concentrations of sodium chloride) then we expect the reaction rate to vary with this density. In the room, consistently with the assumptions at the heart of the filling box process, we assume that all motions are homogeneous, and that diffusive processes are insignificant compared to advection. Therefore, there is no vertical mixing, and no vertical reaction between the various species in the room, and so the evolutions of the various concentrations R_1 , R_2 and R_3 are determined purely by (2.10b).

However, we are also interested in understanding how the various species vary with height within the plume. We consider as an example the flux of species one in the plume through a particular level within the room, which must satisfy

$$\frac{\partial}{\partial z}[P_1 Q] = 2R_1 \alpha M^{1/2} - \frac{Q^2}{M} K P_1 P_2. \tag{2.11}$$

The first term on the right-hand side of (2.11) quantifies the entrainment by the plume of species one from the room fluid (with concentration R_1) while the second term quantifies the loss of species one due to reaction, using the definition of the plume velocity, $w_p = M/Q$. Using the product rule on the left-hand side of (2.11) and rearranging, we can then derive an equation for the spatial variation of species one in the rising plume:

$$\frac{\partial P_1}{\partial z} = \frac{2\alpha M^{1/2}}{Q}(R_1 - P_1) - K \frac{Q}{M} P_1 P_2. \tag{2.12}$$

Analogous equations can naturally be derived for the other species within the plume, yielding

$$\frac{\partial P_2}{\partial z} = \frac{2\alpha M^{1/2}}{Q}(R_2 - P_2) - K \frac{Q}{M} P_1 P_2, \tag{2.13}$$

$$\frac{\partial P_3}{\partial z} = \frac{2\alpha M^{1/2}}{Q}(R_3 - P_3) + K \frac{Q}{M} P_1 P_2. \tag{2.14}$$

As in the dynamic filling box process, inherent in this model is a quasi-steady approximation, in that we assume that the room concentration of the various species does not vary appreciably during the vertical propagation of a particular fluid parcel in the plume. Comparing the typical transit time of a fluid parcel, using the velocity estimates at the ceiling derived from the similarity solution (2.6) to the inverse of the reaction rate (scaled with the maximum concentrations of species one and two) yields the condition

$$\left(\frac{5}{6\alpha}\right) \left(\frac{9\alpha B_0}{10}\right)^{1/3} \gg K H^{4/3} \sqrt{R_{20} P_{10}}. \tag{2.15}$$

2.4. Well-mixed models

The isolated source within the room inevitably leads to vertical variations in both density and species concentration within the room. However, particularly when the source volume flux is small compared to the volume flux of the plume when it arrives at the ceiling (and hence significant entrainment occurs during the plume evolution towards the ceiling), the developing layers can be well-approximated by well-mixed

layers (see CW02 for a fuller discussion). Assuming that the room is completely well-mixed leads to simple models for the evolution of the densities and species within the room. The time evolution of the well-mixed density ρ_W within the room must satisfy the equation

$$\frac{d}{dt}(A_c H \rho_W) = \pi \rho_s Q_s - \pi \rho_W Q_s, \quad \rho_W(0) = \rho_{R0}, \quad (2.16)$$

since the source continually supplies fluid of density ρ_s with the same volume flux as the well-mixed fluid which leaves through the external opening. Therefore, under this assumption, the well-mixed fluid within the room is predicted to converge exponentially to the density of the source fluid:

$$\frac{\rho_{R0} - \rho_W}{\rho_{R0} - \rho_s} = 1 - \exp\left[\frac{-\pi Q_s}{A_c H} t\right]. \quad (2.17)$$

Similar reduced models can be derived for well-mixed concentrations W_1 , W_2 and W_3 for each of the three species. For species one (input at the source) we obtain

$$\frac{d}{dt}(A_c H W_1) = -K A_c H W_1 W_2 + \pi Q_s (P_{10} - W_1), \quad W_1(0) = 0 \quad (2.18)$$

since there is initially none of this species in the room, there is a constant flux (with concentration P_{10} by definition) from the source, and there are losses due to reaction with species two and outflow of the well-mixed concentration through the source. Similar equations for W_2 and W_3 are

$$\frac{d}{dt}(A_c H W_2) = -K A_c H W_1 W_2 - \pi Q_s W_2, \quad W_2(0) = R_{20}, \quad (2.19)$$

$$\frac{d}{dt}(A_c H W_3) = K A_c H W_1 W_2 - \pi Q_s W_3, \quad W_3(0) = 0, \quad (2.20)$$

showing that W_2 decreases from its original value of R_{20} due to both reaction and outflow, while W_3 increases due to reaction provided the other two species are present, but decreases due to outflow. Although these equations do not have a simple solution, it is clear that as $t \rightarrow \infty$, $W_2 \rightarrow 0$ and hence $W_3 \rightarrow 0$ and $W_1 \rightarrow P_{10}$, i.e. the input concentration of species one eventually fills the interior, analogously to the way the room density approaches that of the source fluid. We will be interested in identifying circumstances when these well-mixed models are adequate descriptions of the flow evolution, and also the parameter ranges in which the complexities inherent in the more general filling box description are observable and significant.

2.5. Non-dimensionalization

We now introduce non-dimensional variables (see CW02 for a detailed discussion). The natural length scale to use is the height H of the room. Motivated by the form of the well-mixed density, we scale the density difference from the initial ambient density by the density difference between initial ambient and source fluid, i.e.

$$\hat{z} = \frac{z}{H}, \quad \hat{C}(z, t) = \frac{\rho - \rho_{R0}}{\rho_s - \rho_{R0}}. \quad (2.21)$$

Therefore, for the plume fluid at the source the fluid density concentration $\hat{C}_p(0, t) = 1$, while initially for the ambient fluid in the room, the fluid density concentration $\hat{C}_r(z, 0) = 0$. It is natural to scale the volume flux with its source value Q_s , and the

buoyancy flux with its initial value B_0 , i.e.

$$\hat{Q}(z, t) = \frac{Q}{Q_s}, \quad \hat{Q}(0, t) = 1, \tag{2.22}$$

$$\hat{B}(z, t) = \frac{B}{B_0}, \quad \hat{B}(0, t) = 1 - \hat{C}_R(0, t). \tag{2.23}$$

As observed above, requiring the source density to be constant as in this model, with a non-zero source volume flux, implies that the source buoyancy flux can drop from its initial value as the first front reaches the floor of the room (and so $\hat{C}_R(0, t) > 0$), which must happen in finite time if the source has non-zero source volume flux and the external opening is at the same height as the source.

From comparison with the point-source similarity solution (2.6) discussed above, the source volume flux Q_s can be used to define a so-called ‘effective origin’ (see Caulfield & Woods 1995; Hunt & Kaye 2001) z_e :

$$Q_s = \frac{6\alpha}{5} \left(\frac{9\alpha B_0}{10} \right)^{1/3} z_e^{5/3}, \tag{2.24}$$

i.e. z_e is the notional location below $z = 0$ of a point source with buoyancy flux B_0 which would have volume Q_s at $z = 0$ given by the similarity solution (2.6). Clearly, this point source would also have a particular momentum flux M_{ss} at $z = 0$ given by the similarity solution, where

$$M_{ss} = \left(\frac{9\alpha B_0}{10} \right)^{2/3} z_e^{4/3}. \tag{2.25}$$

We use this characteristic scale M_{ss} to non-dimensionalize the momentum flux, and so

$$\hat{M} = \frac{M}{M_{ss}}, \quad \hat{M}(0, t) = \hat{M}_s. \tag{2.26}$$

If $\hat{M}_s > 1$ the source has an excess of momentum flux above the point-source similarity solution, and so it is commonly referred to as a forced plume. This is equivalent to the source either having too small a source radius, or too large a source velocity. Conversely, if $\hat{M}_s < 1$, the source has a deficit of momentum flux, and it is referred to either as a distributed (Caulfield & Woods 1995) or lazy plume (Hunt & Kaye 2001) as this deficit is equivalent either to a large source radius or a small source velocity. Finally, if $\hat{M}_s = 1$, the plume is said to be in pure plume balance (see Caulfield & Woods 1995) and the plume follows the similarity solution (2.6) for all time (with z replaced by the offset $z + z_e$).

Since the source volume flux is essential to the flow dynamics, the natural time scale of the fluid flow is the fluid replacement time or turnover time scale t_r , defined as

$$t_r = \frac{A_c H}{\pi Q_s}, \tag{2.27}$$

i.e. the time required by the source to replace completely the fluid within the room in the absence of entrainment, and so we define $\hat{t} = t/t_r$. This is also the characteristic time scale of the well-mixed model, as is clear from (2.17), which can be written in terms of a well-mixed fluid density concentration \hat{C}_w as

$$\hat{C}_w = 1 - e^{-\hat{t}}. \tag{2.28}$$

However, it is important to appreciate that all the chemical species within the room may not converge to their steady states on the replacement time scale, particularly in situations where the reaction rate is relatively fast, and so reaction plays a dominant effect in determining the time scale for the chemical species, rather than the (finite volume flux) filling box flow dynamics. We discuss this in more detail below, particularly in §3.

For the chemical concentrations, as already noted, the natural scaling is the geometrical mean of the two initial concentrations, and so we non-dimensionalize as follows:

$$[\hat{R}_1(\hat{z}, \hat{t}), \hat{R}_2(\hat{z}, \hat{t}), \hat{R}_3(\hat{z}, \hat{t})] = \frac{(R_1, R_2, R_3)}{\sqrt{P_{10}R_{20}}}, \quad (2.29)$$

$$[\hat{P}_1(\hat{z}, \hat{t}), \hat{P}_2(\hat{z}, \hat{t}), \hat{P}_3(\hat{z}, \hat{t})] = \frac{(P_1, P_2, P_3)}{\sqrt{P_{10}R_{20}}}, \quad (2.30)$$

with initial and boundary conditions

$$\hat{R}_1(\hat{z}, 0) = \hat{R}_3(\hat{z}, 0) = 0, \quad \hat{R}_2(\hat{z}, 0) = \sqrt{\frac{R_{20}}{P_{10}}} \equiv \phi, \quad (2.31a)$$

$$\hat{P}_2(0, \hat{t}) = \hat{P}_3(0, \hat{t}) = 0, \quad \hat{P}_1(0, \hat{t}) = \frac{1}{\phi}. \quad (2.31b)$$

with $\hat{R}_1 = R_1/\sqrt{P_{10}R_{20}} \rightarrow \sqrt{P_{10}/R_{20}} = 1/\phi$ and $\hat{R}_2 \rightarrow 0$ as $\hat{t} \rightarrow \infty$. We also use $\sqrt{R_{20}P_{10}}$ and t_r to define a non-dimensional reaction rate λ as

$$\lambda = \frac{K\sqrt{R_{20}P_{10}}A_cH}{\pi Q_s}, \quad (2.32)$$

where it is important to remember that, since λ can be a function of temperature and ionic strength, it may depend on the local values of the fluid density, or equivalently fluid density concentration. Using this scaling, the quasi-steady approximation for the reaction (2.15) takes the form (using (2.7) and (2.24))

$$\frac{\theta}{\hat{z}_e^{5/3}\lambda} \gg 1, \quad (2.33)$$

which is clearly related to the quasi-steady approximation condition (2.7) for the validity of the filling box process.

Using these natural scalings, the plume equations may be rewritten as

$$\frac{\partial \hat{Q}}{\partial \hat{z}} = \frac{5}{3\hat{z}_e} \hat{M}^{1/2}, \quad (2.34a)$$

$$\frac{\partial \hat{M}}{\partial \hat{z}} = \frac{4}{3\hat{z}_e} \frac{\hat{B}\hat{Q}}{\hat{M}}, \quad (2.34b)$$

$$\frac{\partial \hat{B}}{\partial \hat{z}} = -\hat{Q} \frac{\partial \hat{C}_R}{\partial \hat{z}}, \quad (2.34c)$$

with the boundary conditions, as already noted,

$$\hat{Q}(0, t) = 1, \quad \hat{M}(0, t) = \hat{M}_s, \quad \hat{B}(0, t) = 1 - \hat{C}_R(0, t). \quad (2.35)$$

If the ambient concentration is constant and zero, and $\hat{M}_s = 1$ so that the plume is in pure plume balance, the similarity solution (2.6) takes the form

$$\hat{Q} = \left(\frac{\hat{z} + \hat{z}_e}{\hat{z}_e} \right)^{5/3}, \quad \hat{M} = \left(\frac{\hat{z} + \hat{z}_e}{\hat{z}_e} \right)^{4/3}. \quad (2.36)$$

The equation for the evolution of the ambient density in the room (2.4) becomes

$$\frac{\partial \hat{C}_R}{\partial \hat{t}} = \hat{Q} \frac{\partial \hat{C}_R}{\partial \hat{z}}, \quad \hat{C}_R(\hat{z}, 0) = 0. \quad (2.37)$$

Similarly, the equations for the evolution of the chemical species in the room (2.10*b*) and in the isolated source (2.12)–(2.14) become respectively

$$\frac{D\hat{R}_1}{D\hat{t}} = -\lambda \hat{R}_1 \hat{R}_2, \quad (2.38a)$$

$$\frac{D\hat{R}_2}{D\hat{t}} = -\lambda \hat{R}_1 \hat{R}_2, \quad (2.38b)$$

$$\frac{D\hat{R}_3}{D\hat{t}} = \lambda \hat{R}_1 \hat{R}_2, \quad (2.38c)$$

and

$$\frac{\partial \hat{P}_1}{\partial \hat{z}} = \frac{5}{3\hat{z}_e} (\hat{R}_1 - \hat{P}_1) - \frac{\lambda \hat{z}_e^2}{\theta} \frac{\hat{Q}}{\hat{M}} \hat{P}_1 \hat{P}_2, \quad (2.39a)$$

$$\frac{\partial \hat{P}_2}{\partial \hat{z}} = \frac{5}{3\hat{z}_e} (\hat{R}_2 - \hat{P}_2) - \frac{\lambda \hat{z}_e^2}{\theta} \frac{\hat{Q}}{\hat{M}} \hat{P}_1 \hat{P}_2, \quad (2.39b)$$

$$\frac{\partial \hat{P}_3}{\partial \hat{z}} = \frac{5}{3\hat{z}_e} (\hat{R}_3 - \hat{P}_3) + \frac{\lambda \hat{z}_e^2}{\theta} \frac{\hat{Q}}{\hat{M}} \hat{P}_1 \hat{P}_2, \quad (2.39c)$$

with initial and boundary conditions

$$\hat{P}_1(0, \hat{t}) = \frac{1}{\phi}, \quad \hat{P}_2(0, \hat{t}) = \hat{P}_3(0, \hat{t}) = 0, \quad (2.40a)$$

$$\hat{R}_2(\hat{z}, 0) = \phi, \quad \hat{R}_1(\hat{z}, 0) = \hat{R}_3(\hat{z}, 0) = 0. \quad (2.40b)$$

It is apparent by using (2.36) at $\hat{z} = 1$ that the quasi-steady assumption for the chemically reacting species (2.33) corresponds to requiring that the second terms on the right-hand side of (2.39) be appropriately small. Finally, the well-mixed equations (2.18)–(2.20) for the various chemical species become

$$\frac{d\hat{W}_1}{d\hat{t}} = \frac{1}{\phi} - \hat{W}_1 - \lambda \hat{W}_1 \hat{W}_2, \quad \hat{W}_1(0) = 0, \quad (2.41a)$$

$$\frac{d\hat{W}_2}{d\hat{t}} = -\hat{W}_2 - \lambda \hat{W}_1 \hat{W}_2, \quad \hat{W}_2(0) = \phi, \quad (2.41b)$$

$$\frac{d\hat{W}_3}{d\hat{t}} = -\hat{W}_3 + \lambda \hat{W}_1 \hat{W}_2, \quad \hat{W}_3(0) = 0. \quad (2.41c)$$

Two particular limiting solutions of these equations are useful for understanding the time scales of the evolution of the reacting species within the flow, particularly in the circumstances which we consider experimentally. First, if $\lambda \hat{W}_2 \ll 1$, which is certainly always true when $\lambda \phi \ll 1$, then, under the further simplifying assumption

that the reaction rate is independent of the local density,

$$\hat{W}_{1a} \simeq \frac{1}{\phi}(1 - e^{-\hat{t}}), \quad (2.42a)$$

$$\hat{W}_{2a} \simeq \phi \exp \left[- \left(\hat{t} + \frac{\lambda}{\phi} [\hat{t} - 1 + e^{-\hat{t}}] \right) \right]. \quad (2.42b)$$

This corresponds to a situation where the concentration of species two is always very low, and the reaction is pseudo-first-order, with the concentration of species two limiting the reaction of the input species one. The other limiting case is $\lambda \hat{W}_1 \ll 1$ (definitely the case initially, but true for all time if $\lambda/\phi \ll 1$), where once again if we assume that λ is independent of the local density,

$$\hat{W}_{1b} \simeq \frac{1 - \exp[-(t + \lambda\phi[1 - e^{-\hat{t}}])]}{\phi} - \lambda[E_1(\lambda\phi e^{-\hat{t}}) - E_1(\lambda\phi)] \exp[-t + \lambda\phi e^{-\hat{t}}], \quad (2.43a)$$

$$\hat{W}_{2b} \simeq \phi e^{-\hat{t}}, \quad (2.43b)$$

where $E_1(v)$ is the exponential integral, (see Abramowitz & Stegun 1965) defined, for positive v , as

$$E_1(v) = \int_v^\infty \frac{e^{-u}}{u} du. \quad (2.44)$$

This solution has the correct asymptotic behaviour of \hat{W}_1 increasing towards $1/\phi$ as $\hat{t} \rightarrow \infty$. For this limit always to apply, since $\phi \gg 1$, the concentration of species one is always very much less than species two, and the reaction is again pseudo-first-order, now limited by the (low) concentration in the incoming plume fluid.

For both of these limits, the concentrations of the reacting chemical species are predicted to approach their asymptotic values on the fluid replacement time scale t_r , at least to leading order. The reaction, because of the (assumed) wide disparity in the concentrations of the two species is a higher-order effect. This is because the evolution of the chemical species is dominated by the volume flux into and out of the room (just as the well-mixed fluid density concentration \hat{C}_w defined in (2.28) is) rather than by the chemical reaction, which is 'slow' in some sense, because the limiting assumptions are only satisfied if the reaction rate λ is relatively small. As can be seen from (2.41), it is not immediately clear whether the replacement time scale is the natural time scale for reactions with larger λ , consistent of course with the quasi-steady assumption through satisfying (2.33). To investigate this issue and others, we wish to compare the various well-mixed models both with the predictions of the full models and with the results of laboratory experiments, where, as discussed below, for technical reasons we find it convenient to use extreme values of ϕ (both large and small).

3. Numerical modelling

3.1. Numerical method

We solved the plume evolution equations (2.34), the ambient concentration equation (2.37), the room chemical equations (2.38), and the plume chemical equations (2.39), subject to the boundary and initial conditions (2.35) and (2.40) using the numerical integration scheme of Germeles (1975). With this method the ambient

density and chemical concentrations are discretized into a finite number of layers, separated by sharp interfaces. As already noted, quasi-steady assumptions (2.7) and (2.33) allow us, at every timestep, to solve the spatial evolution equations for the plume dynamical and chemical properties using a fourth-order Runge–Kutta scheme from the given source conditions \hat{z}_e , \hat{M}_s and ϕ to the top of the room with ‘frozen’ ambient profiles of density and chemical species concentration. Any density dependence of the reaction rate λ can be straightforwardly included as the density in the plume at each height is known. We then update the ambient profiles, installing a new layer at the top of the room consisting of the arriving plume fluid, changing the layer depths consistently with the entrainment into the plume (or equivalently the velocity of the various interfaces given by (2.37)). We also evolve the various chemical species within each layer using (2.38), as solving for each of the species in each layer is equivalent to solving the reaction equation following fluid parcels, with the reaction rate determined if necessary by the local density of the fluid layer. We continue to evolve our calculation until the flow reaches its ultimate steady state, with the room completely filled with fluid of source density $\hat{C}_R \rightarrow 1$, and chemical species $\hat{R}_1 \rightarrow 1/\phi$. Typically this occurs over time scales of the order of a few fluid replacement times.

3.2. Parameter ranges

The complete system (2.34), (2.37)–(2.39), with boundary and initial conditions (2.35) and (2.40) is thus described by five parameters: \hat{z}_e and \hat{M}_s which essentially determine the source conditions for the plume; ϕ which determines the source conditions for the chemical species; $\lambda(\hat{C})$ which determines the reaction rate, and which may be a function of the local fluid density concentration; and θ which determines the room aspect ratio. Central to the quasi-steady assumptions necessary for this model is that θ is sufficiently large, and $\lambda\hat{z}_e^{5/3}$ is sufficiently small so that (2.7) and (2.33) are satisfied but there is clearly still a very large parameter space that can be described by this model. We shall follow two guiding principles in our choice of parameters to discuss, without presenting an overwhelming number of studies. As our primary focus is the behaviour of the chemically reacting species, our discussion will focus on the dependence of the system on the two chemically related parameters λ and ϕ . The choices of the other parameters will be restricted to specific values characteristic of physically realistic situations, as we discuss in more detail below.

Although the condition on the aspect ratio parameter θ is implicit in previous studies of non-reacting filling box flows, it does not play an explicit role provided an appropriate non-dimensional formulation is used. Here, however, due to the presence of the competing time-dependent processes of the filling box process and the reaction between the two species, the particular value of θ is essential to the formulation, as it inevitably appears in the equation for the evolution of \hat{P}_i in (2.39). For rooms which are roughly cubic (and so $A_c \sim H^2$) $\theta \sim 20$ – 30 (which is naturally consistent with the quasi-steady approximation), since typical values of the entrainment constant are of the order of $\alpha \sim 0.1$, and so in this section we fix $\theta = 20$.

There are also sensible restrictions which can be placed on the value of the effective origin \hat{z}_e . For at least four reasons it is natural to consider flows where \hat{z}_e is significantly less than 1. First, such flows, where the plume undergoes substantial entrainment before it reaches the top of the enclosed space, are commonplace in environmental and industrial applications. Secondly, such flows are more likely to enable a quasi-steady filling box process to develop. Thirdly, as is well known, such flows are more straightforward to model experimentally (as discussed in more detail below) and therefore are more likely to allow the direct experimental verification of

our theoretical model. Finally, for such flows the well-mixed models are likely to be approximations of at least some utility, and so the comparison between the detailed and more reduced models are likely to be more meaningful. Therefore, in this section we consider $\hat{z}_e = 0.1$.

There are then two natural choices for the source momentum flux \hat{M}_s . First, choosing $\hat{M}_s = 1$ implies that initially the plume is in pure plume balance, and therefore follows the similarity solution defined in (2.36). This is useful for illustrative purposes, has been commonly done previously, and is what we choose to do in this section. A particular attraction of this choice is that an analytical expression can be derived for the non-dimensional arrival time \hat{t}_a of the first front at the source location $\hat{z} = 0$, which, as we see below, is an important separating time in the flow evolution. Indeed, as discussed in more detail in CW02, for the similarity solution (2.36) it is clear that

$$\hat{t}_a \equiv \int_1^0 \frac{d\hat{z}}{\hat{w}_r} = \int_0^1 \frac{d\hat{z}}{\hat{Q}} = \frac{3}{2} \hat{z}_e \left(1 - \left[\frac{\hat{z}_e}{1 + \hat{z}_e} \right]^{2/3} \right), \quad (3.1)$$

which can be significantly less than 1 (and hence dimensionally significantly less than the replacement time scale of the room) when $\hat{z}_e \ll 1$.

It is important to stress that after this time, since the source buoyancy flux drops from its initial value, the plume ceases to be in pure plume balance, and becomes forced, with the source momentum flux playing an increasingly important role as the flow tends towards its steady state with the room completely filled by source fluid, and the source behaving like a pure momentum jet (see CW02 for a more detailed discussion). Furthermore, a possible area for lack of agreement between the various well-mixed models and the detailed plume filling box model is due to the difference of behaviour of the two systems before this time. All the well-mixed models assume from the initial instant that fluid at least slightly affected by the plume (either through having a density less than the initial room density or through having a non-zero concentration of species one) leaves through the vent. However, in reality, fluid that has been cycled through the plume only leaves once the first front reaches the floor, and hence the opening to the exterior. In circumstances where the effective origin $\hat{z}_e \ll 1$, this time is significantly shorter than the characteristic replacement time for the room to approach its final steady state, and so we expect that the influence of this initial mismatch might be small.

The other natural choice for a source condition for the momentum flux is motivated by conventional experimental techniques. For a source of a given area A_s , if it is assumed that the source velocity is constant across this area, then dimensionally $M_s = Q_s^2/A_s$, or equivalently, using the scalings of this paper

$$\hat{M}_s = \frac{A_c}{A_s} \frac{\hat{z}_e^2}{\pi\theta}. \quad (3.2)$$

We use this scaling in §4 when we compare our model to our experiments.

For these particular choices of the parameters governing the plume dynamics, the vertically averaged fluid density concentration \hat{C}_R remains very close to the fluid density concentration \hat{C}_W predicted by the well-mixed model defined in (2.28). In particular, the fluid density evolves on the time scale of the fluid replacement time scale defined in (2.27). Since we wish to focus on the evolution of the chemical species, we do not show the time evolution of the density concentrations in this paper. The time dependence of the vertically averaged concentration is discussed in some detail in CW02. Indeed, these fixed, and reasonable, choices of three of the parameters

allow us to devote our attention to the effect of variations in the chemically related parameters.

Since it is still necessary for our quasi-steady approximation (2.33), λ is restricted such that

$$\lambda \ll \frac{\theta}{\hat{z}_e^{5/3}} \sim 1000, \quad (3.3)$$

for the chosen values of the other parameters. This is not very restrictive, and so to understand the effect of marked variations in λ , we consider the two choices $\lambda = 0.1$ and 10 , both of which still satisfy (3.3). This allows us to investigate what the appropriate time scales for the chemical species are when the reaction rate λ is sufficiently large to be significant compared to the finite volume flux filling box process, which occurs on the fluid replacement time scale. Furthermore, as we discuss in §4, this range is appropriate for the experimental system we considered.

On the other hand, ϕ is not constrained by an essential assumption. However, since we derived above particular explicit reduced models for $\lambda\phi \ll 1$ and $\lambda/\phi \ll 1$ (i.e. (2.42) and (2.43)), we consider the two choices $\phi = 0.1$ and $\phi = 10$. These choices also are of the order that is feasible in the laboratory.

3.3. Vertically averaged results

Since we are interested in the quality of the predictions of the reduced models in comparison to the full numerical model, for each of the four possible combinations of λ and ϕ , we first consider various vertically averaged chemical quantities in the room. In figures 2 and 3, we plot the evolution against time of \hat{R}_i for $i = 1, 2, 3$ where the overbar denotes vertical averaging in the room, for flows with $\phi = 0.1$ and $\phi = 10$ respectively. We also plot the predictions of the various well-mixed models: \hat{W}_i for $i = 1, 2$ as defined by the well-mixed model (2.41); \hat{W}_{ia} for $i = 1, 2$ for the analytical model when $\lambda\hat{W}_2 \ll 1$ as defined in (2.42); and \hat{W}_{ib} for $i = 1, 2$ for the analytical model when $\lambda\hat{W}_1 \ll 1$ as defined in (2.43). We expect \hat{W}_{ia} to be most applicable when $\lambda = 0.1$, $\phi = 0.1$, (i.e. figures 2*a* and 2*c*) and \hat{W}_{ib} to be most applicable when $\lambda = 0.1$, $\phi = 10$ (i.e. figures 3*a* and 3*c*). Because of the wide disparity, for these values of ϕ , between the initial values of $\hat{R}_2 = \phi$ and the final values of $\hat{R}_1 = 1/\phi$, we plot \hat{R}_3 (using a thick solid line) for each of the four flows on the panel with the smallest vertical extent: i.e. with \hat{R}_2 when $\phi = 0.1$ in figure 2, and with \hat{R}_1 when $\phi = 10$ in figure 3. This is because the magnitude of the concentration of the reaction product will naturally be determined by the lesser magnitude of the concentrations of the reactants.

In general, it is clear from the figure that the concentration of species one (initially input from the source) within the room approaches its steady state value (of $1/\phi$) on the time scale of a few fluid replacement time scales. The only exception to this observation appears to be shown in figure 3(*b*). This is due to the effect of a large reaction rate (i.e. $\lambda \gg 1$) and a significantly larger initial concentration of species two in the room, thus leading to initial suppression in the rate of increase of species one within the room, until all species two is lost. Since there is a large initial concentration of species two, this takes a relatively long time.

Analogously, species two appears to drop to zero on the same time scale except in the case where there is a small initial concentration (i.e. $\phi \ll 1$) and the reaction rate is high, as shown in figure 2(*d*). This is unsurprising, as the large reaction rate rapidly depletes the small initial room concentration of species two in this case. The effect of high reaction rate is also apparent in the evolution of the product species three,

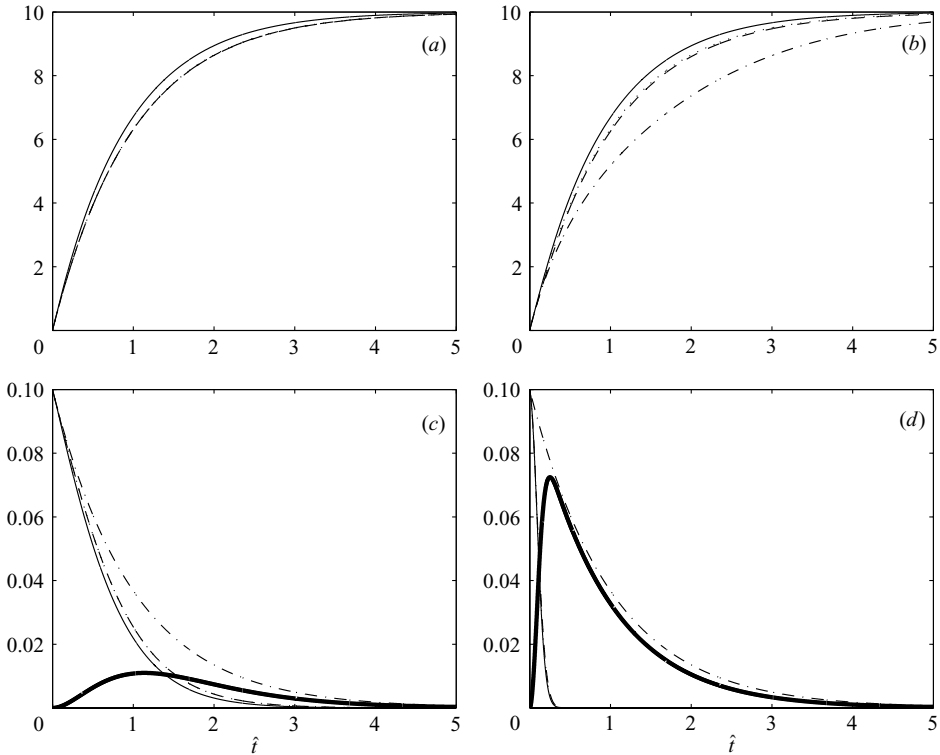


FIGURE 2. (a, b) Variation with time of vertically averaged concentrations \hat{R}_1 (plotted with a solid line), \hat{W}_1 as defined by (2.41) (dashed line), \hat{W}_{1a} as defined by (2.42) (dotted line), and \hat{W}_{1b} as defined by (2.43) (dot-dashed line), for flows with $\hat{M}_s = 1$, $\hat{z}_e = 0.1$, $\theta = 20$, $\phi = 0.1$ and (a) $\lambda = 0.1$; (b) $\lambda = 10$. (c, d) Variation with time of vertically averaged concentrations \hat{R}_2 (plotted with a solid line), \hat{R}_3 (thick solid line), \hat{W}_2 as defined by (2.41) (dashed line), \hat{W}_{2a} as defined by (2.42) (dotted line), and \hat{W}_{2b} as defined by (2.43) (dot-dashed line), for flows with $\hat{M}_s = 1$, $\hat{z}_e = 0.1$, $\theta = 20$, $\phi = 0.1$ and (c) $\lambda = 0.1$; (d) $\lambda = 10$.

whose peak value is substantially higher in the cases of large λ (figures 2d and 3c) than when $\lambda \ll 1$.

It is also apparent that the well-mixed models capture much of the character of the evolution of the concentrations within the room when they are expected to be relevant (i.e. figures 2a and 3a) for the range of parameter choices presented. On the other hand, \hat{W}_{1a} is a very poor approximation when $\lambda = 10$, $\phi = 10$ (i.e. the dotted line in figure 3b). This is unsurprising, since this choice of parameters violates strongly the assumption for this reduced well-mixed model, namely that $\lambda\phi \ll 1$. However, there is a clear systematic error, with at a given time the well-mixed models over-estimating \hat{R}_2 and underestimating \hat{R}_1 . This can be straightforwardly understood from consideration of the behaviour of the system at early times. The well-mixed models assume that some species one (input by the source in fact) is vented from the opening at the floor of the room from the very first instant. Therefore, the well-mixed models assume that the vented fluid has concentration of species two less than its original concentration. However, until the first front has reached the floor of the room, none of species one is actually vented, and all the fluid which is vented has the initial room concentration of species two. Although, for the choice of the parameters

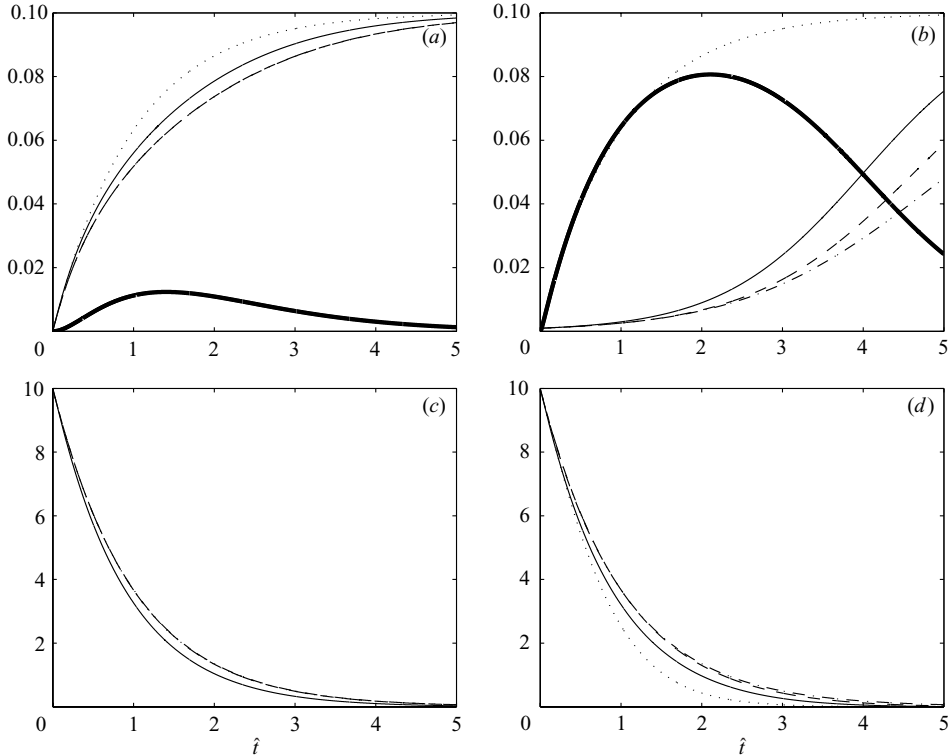


FIGURE 3. (a, b) Variation with time of vertically averaged concentrations \bar{R}_1 (plotted with a solid line), \hat{R}_3 (thick solid line), \hat{W}_1 as defined by (2.41) (dashed line), \hat{W}_{1a} as defined by (2.42) (dotted line), and \hat{W}_{1b} as defined by (2.43) (dot-dashed line), for flows with $\hat{M}_s = 1$, $\hat{z}_e = 0.1$, $\theta = 20$, $\phi = 10$ and (a) $\lambda = 0.1$; (b) $\lambda = 10$. (c, d) Variation with time of vertically averaged concentrations \hat{R}_2 (plotted with a solid line), \hat{W}_2 as defined by (2.41) (dashed line), \hat{W}_{2a} as defined by (2.42) (dotted line), and \hat{W}_{2b} as defined by (2.43) (dot-dashed line), for flows with $\hat{M}_s = 1$, $\hat{z}_e = 0.1$, $\theta = 20$, $\phi = 10$ and (c) $\lambda = 0.1$; (d) $\lambda = 10$.

presented here the arrival time, as defined in (3.1), is $\hat{t}_a = 0.1197 \ll 1$, nevertheless the initial period leads to the well-mixed models overpredicting the amount of species one and underpredicting the amount of species two vented from the room. This leads to the observed underprediction of species one within the room, and overprediction of species two within the room. For the particular parameter choices shown, there is typically little difference between the numerical and analytical well-mixed models defined by (2.41)–(2.43).

The evidence points to the fluid replacement time scale also being an appropriate time scale for the chemical concentrations within the room, a fact that can also be deduced from the reduced models, except when $\lambda \gg 1$. However, an important aspect of the flow (particularly for application to hazard analysis) is the dependence of the (product) species three on the two chemical parameters: i.e. non-dimensional initial room concentration ϕ and the reaction rate λ . As can be observed qualitatively in figures 2 and 3, increasing λ leads to a larger peak value of \hat{R}_3 , while increasing ϕ leads to the later occurrence of this peak. To understand this behaviour quantitatively, and also to identify the relevance of the well-mixed model concentration \hat{W}_3 defined by (2.41c), in figure 4 we plot the peak values of \hat{R}_3 and \hat{W}_3 , and the (non-dimensional)

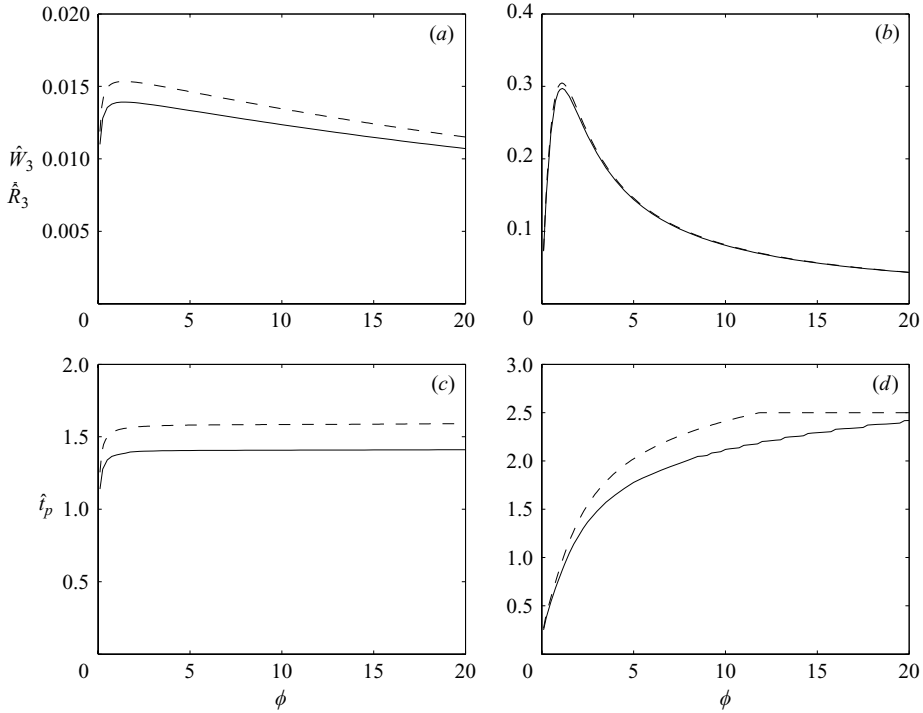


FIGURE 4. (a, b) Variation with ϕ of the peak value of the vertically averaged concentration \hat{R}_3 of the chemical product (plotted with a solid line), and the well-mixed concentration \hat{W}_3 as defined by (2.41) (dashed line), for flows with $\hat{M}_s = 1$, $\hat{z}_e = 0.1$, $\theta = 20$, and (a) $\lambda = 0.1$; (b) $\lambda = 10$. (c, d) Variation with ϕ of the time \hat{t}_p for the occurrence of the peak value of the vertically averaged concentration \hat{R}_3 of the chemical product (plotted with a solid line), and the time for the occurrence of the peak value of the well-mixed concentration \hat{W}_3 as defined by (2.41) (dashed line), for flows with $\hat{M}_s = 1$, $\hat{z}_e = 0.1$, $\theta = 20$, and (c) $\lambda = 0.1$; (d) $\lambda = 10$.

time \hat{t}_p of occurrence of this peak against ϕ for the two values $\lambda = 0.1$ and $\lambda = 10$ used in figures 2 and 3.

Certain characteristics are apparent. As already noted, larger values of λ correspond to larger peak values of the product concentration, unsurprisingly, since larger values of λ imply more vigorous reaction before the filling box process leads to loss of the finite quantity of species two (initially in the room) through the external vent. There is also a clear non-monotonic variation of the peak value with ϕ for a given value of λ , with a maximum occurring around $\phi \sim 1$. For small values of ϕ , the concentration of the product species three is limited by the initial concentration ϕ of species two in the room. In particular if ϕ is very small, it is rapidly depleted by any reaction and the peak concentration of species three occurs at a very small value. On the other hand, for large values of ϕ , the concentration of species three is limited by the source concentration $1/\phi$ of species one entering the room through the source, and in particular when λ is large, the peak concentration of species three exhibits a $1/\phi$ dependence at large ϕ .

Turning attention to the usefulness of the well-mixed model, for both values of λ shown, \hat{W}_3 over-estimates the actual peak value of the product chemical species concentration, although the well-mixed model does appear to be a good

approximation, particularly when $\lambda = 10$ (figure 4). This over-estimation is principally due to the fact, as noted above, that the well-mixed model over-estimates the concentration of species two, i.e. the species initially within the room. Since more of species two is assumed to remain within the room by the well-mixed model, more reaction is assumed to take place than actually occurs within the full model. This effect is not so significant for larger values of λ as, for flows with higher reaction rates, differences in the evolution of species two between the well-mixed model and the full model are not so important, and the evolution is more strongly determined by the reaction rate.

The time \hat{t}_p for the occurrence of the peak value of the product species three concentration also exhibits qualitatively different behaviour for small and large values of ϕ . For smaller values of λ (figure 4c), this time is essentially constant, and of the order of the fluid replacement time except when ϕ is very small. When ϕ is very small of course, species two is rapidly depleted, and so the reaction ends very early. However, for larger values of ϕ the chemical species concentrations within the flow evolve on the filling box replacement time scale, and so the time to peak concentration varies only weakly with ϕ . The well-mixed model systematically over-estimates \hat{t}_p , due as usual to the fact that it systematically over-estimates the amount of species two remaining in the room, and thus the potential for further reaction to take place between the incoming source fluid (containing only species one) and the finite quantity of species two.

For larger values of λ (as shown in figure 4d) \hat{t}_p behaves in a qualitatively different manner, both in not being so strongly determined by the fluid replacement time scale (which has been used in the non-dimensional scheme, and thus corresponds to $\hat{t}_p = 1$) and also in showing a strong dependence on ϕ . For smaller values of ϕ , increasing λ actually reduces \hat{t}_p . As is apparent in figure 2, when ϕ is small, and so the reaction is limited by the concentration of species two initially in the room, high reaction rates rapidly deplete this species, and so product species three reaches its maximum concentration very quickly, in a manner that does not depend strongly on the filling box process. Conversely, when ϕ is large, the reaction is limited by the low incoming source concentration $1/\phi$ of species one. For flows with higher reaction rates, peak concentrations of the product species three can occur even after significant loss of species two through the external opening, (due to the filling box process) since the cumulative input of species one associated with the large initial concentration of species two in the room can lead to more efficient reaction than in flows with smaller values of λ . Nevertheless, the peak concentration of the reaction species still occurs within a relatively small number of fluid replacement times, as inevitably species two will all be lost from the room through the external opening, as source fluid completely fills the room.

3.4. Vertical profile results

We are not only interested in vertically averaged outputs from our models, but also in the time-dependent behaviour of vertical profiles of the various flow quantities of interest. In figures 5 and 6, we plot vertical profiles for each of the four quantities of interest (\hat{C}_R and \hat{R}_i for $i = 1, 2, 3$) at evenly spaced time intervals $\hat{t}_j = j/5$; $j = 1, 2, 3, \dots$, i.e. at intervals of 20% of the fluid replacement time t_r defined by (2.27) for the same parameter choices considered in figures 2 and 3 respectively. Similarly to the fluid density concentration profile \hat{C}_R as considered previously in CW02, each of the profiles shows a clear vertical concentration gradient, strongest

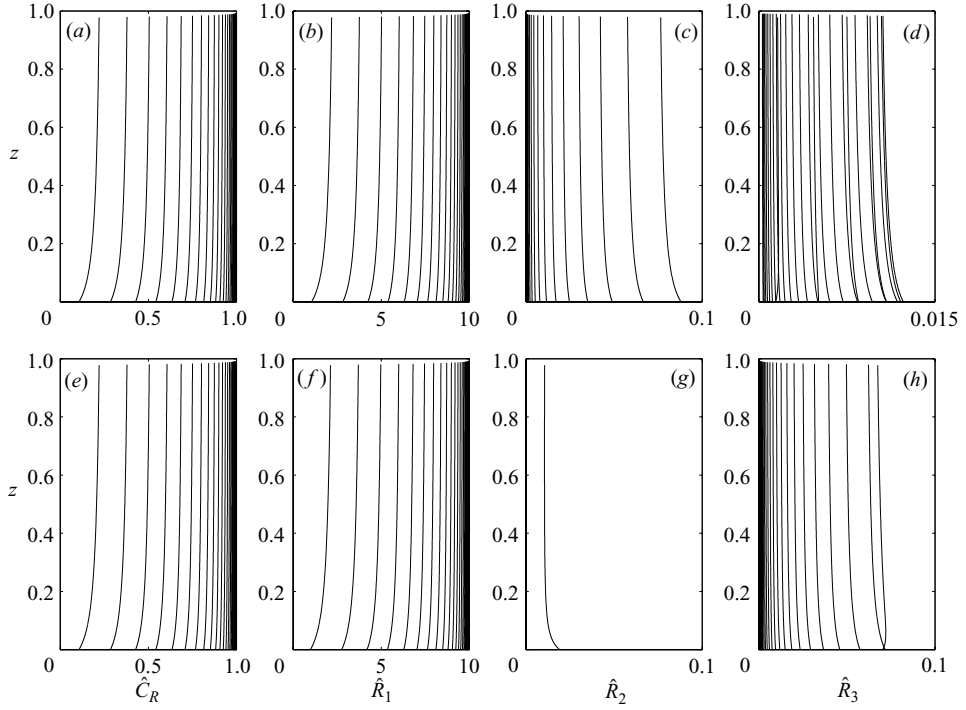


FIGURE 5. Concentration profiles as a function of height at times $\hat{t}_j = j/5$; $j = 1, 2, 3 \dots$ for: \hat{C}_R (a, e); \hat{R}_1 (b, f); \hat{R}_2 (c, g); \hat{R}_3 (d, h). In all cases $\hat{M}_s = 1$, $\hat{z}_e = 0.1$, $\theta = 20$, and $\phi = 0.1$ while $\lambda = 0.1$ in a-d; $\lambda = 10$ in e-h.

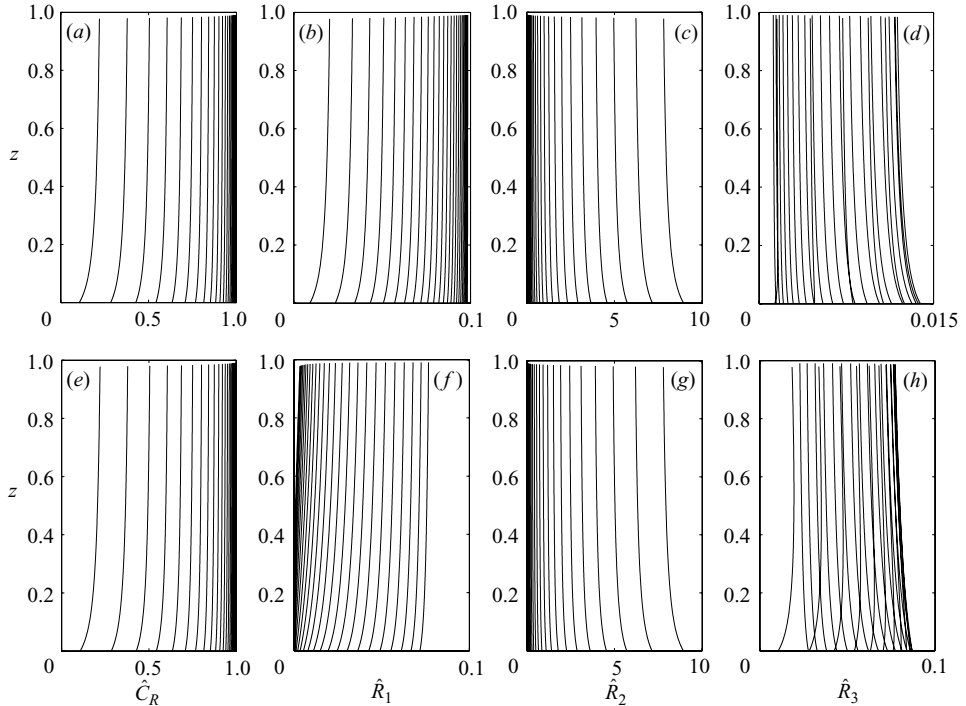


FIGURE 6. As figure 5 but for $\phi = 10$.

near the floor of the room. In each case, the gradient approaches zero over time. Unsurprisingly, it is clear that, when $\lambda = 10$ and $\phi = 0.1$, so that both the reaction is fast and the initial concentration of \hat{R}_2 is small, the room is rapidly depleted of species two, as shown in figure 5(g). Also, it is clear in the last column (figures 5d, 5h, 6d and 6h) that \hat{R}_3 increases from zero in the room as reactions take place, and then drops towards zero as species two is completely depleted.

Interestingly, species one (the species input from the source) and species two (the species initially in the room) are qualitatively different in their vertical structure. Species one is similar to the density concentration, in that it has the smallest value near the floor of the room, increasing towards the ceiling. This is unsurprising, as both enter the room through the plume. As the flow evolves, and the plume rises through and re-entrains fluid that has already been cycled through the plume, the concentration of both fluid density and species one in the plume as it reaches the ceiling (and spreads out as a new layer) must increase, thus leading to a positive vertical gradient. Conversely, the concentration of species two is greater near the floor of the room, since species two is originally in the room alone. Therefore, the layers within the room which have had a longer residence time, and have been less affected by the plume, will tend to have higher concentrations of species two. These layers naturally are closer to the floor.

Finally, the product species three exhibits aspects of both of these behaviours. At early times, when both species one and species two are present in non-trivial quantities, vertical profiles of species three behave like those of species one, with higher concentrations at higher points in the room. This is due to the fact that fluid cycled through the plume is accessing sufficient quantities of species two to lead, through reaction, to creation of the product species three. Therefore, more recently created layers, near the ceiling of the room, will have higher concentrations of species three. However, eventually species two becomes depleted, and so less and less creation of the product species three occurs. The older layers (which were generated when reaction was more prevalent) have higher concentrations of species three. Therefore, at later times, profiles of species three are similar to those of species two, with greater concentrations closer to the floor of the room. Having developed these models, we now investigate whether their predictions agree with the results of analogue laboratory experiments.

4. Experiments

4.1. Experimental method

We conducted the experiments in a Plexiglas tank (43 cm \times 28 cm \times 28.8 cm) open to the exterior at the upper surface with two evenly spaced holes drilled in the tank bottom. The first hole contained a plume source, located far enough away from the walls so that $A_c \gg b^2$ at all heights within the plume. The source consisted of a small tube connected to an expansion chamber with a pin-sized hole on the upstream side, following a design originally due to Dr Paul Cooper (see Hunt & Linden 2001 for a more detailed description of the design). On the downstream side of the chamber is plastic gauze leading to a 5 mm diameter orifice, through which the final discharge occurs. The flow is essentially turbulent on exit. A tank mounted at the ceiling of the laboratory supplied the source. The level of the supply tank was maintained by a pump and overflow system connected to a larger tank located on the floor, and

hence the hydrostatic pressure head between the supply tank and experimental tank was constant. During the experiment the pump was only turned on intermittently so as to not increase the fluid temperature, as the reaction rate of the chemical species which we used is strongly sensitive to temperature. The second hole in the experimental tank was connected to a vertical tube opening to the exterior air. The level of the top of this tube was modified until a hydrostatic balance was reached with the fluid inside the experimental tank, such that throughout the entire course of the experiment, the depth of fluid in the experimental tank remained constant, with extremely small fluctuations. Therefore, we were confident that the flows into and out of the experimental tank were constant and equal to Q_s (which we were able to modify).

Density variations between the plume fluid and the room were caused in the conventional way by varying the concentration of sodium chloride in the room fluid initially. In all cases, the source fluid had no salt content, and so was buoyant relative to the initial room fluid, whose density could be varied experimentally. The two chemical species used in the experiments were malachite green, a triphenylmethane dye, and sodium hydroxide, a strong base. In the presence of a strong base the malachite green, which is green in solution, bonds with the hydroxide anion to form a colourless molecule. There are three reasons why these two species are appropriate for an experimental verification of our model. First, the reaction rate is sufficiently slow for the quasi-steady assumption to be valid for the range of concentrations that we consider. Secondly, although there is some energy release during the reaction, it can be shown to be sufficiently small to have a negligible effect on the fluid density and reaction rate. Finally, it is straightforward to measure quantitatively changes in colour of the solution experimentally, and thus to measure the changing concentration of one of the chemical species with time.

We lit the experimental apparatus uniformly from one side, and videoed the experimental tank through the other side using a digital monochrome CCD camera. The light intensity of this image then acts as a proxy for the coloured dye still remaining in the tank, and hence the concentration of one of the chemically reacting species, when the time sequence of images is analysed with appropriate image analysis software. We used the package DigImage (see for example Dalziel 1993) and so we were able to measure how both vertical profiles and the mean concentration of one of the species varied with time. In most experiments, we used malachite green as species one, and so the source contained only malachite green, while the room initially had a non-zero concentration of sodium hydroxide (as species two). In this case, we tracked how the light intensity changed as the room approached being filled with green fluid alone. However, we also considered the reversed situation, where the source had a non-trivial concentration of sodium hydroxide, and the room was initially filled with some concentration of malachite green. In this case we were able to track how the colour decreased in the room as both reaction and outflow through the opening led to the loss of malachite green.

Essential to this experimental technique is of course the calibration of light intensity with concentration of the malachite green chemical species. We determined this by placing a known concentration, determined on a mass basis, in the tank, and then recording the measured light intensity. This process was repeated about 20 different times between the maximum concentration used in the experiment and the smallest concentration distinguishable by the camera.

For the comparison of our experimental results with our theoretical models, it was also necessary to determine the (dimensional) rate constant K , which needs to be

Experiment	\hat{z}	\hat{M}_s	ϕ	θ	λ	ρ_R (kg m ⁻³)
A	0.054	0.176	10	32.1	1.05K	1.001
B	0.054	0.176	15.1	32.1	1.38K	1.05
C	0.054	0.176	0.0644	32.1	1.42K	1.02

TABLE 1. Non-dimensional constants and initial fluid density in the tank for each experiment performed. The values for λ are multiplied by the rate constant K , which varies between 0.3 and 1.2 depending on the salinity.

considered carefully. Although sodium chloride, which as noted above was used to increase the density of the ambient fluid, does not have a significant side reaction with the reacting chemical species, its presence does increase the ionic strength of the solution, and thus decreases the rate constant of the reaction. Since the concentration of salt in the tank changes with time we needed to determine experimentally how the rate constant varied with salt concentration. Also, K is unsurprisingly a strong function of temperature. Therefore, through each experiment we carefully monitored the fluid temperature, and minimized temperature fluctuations. The peak variation in temperature was always less than 0.5 °C.

To determine the functional form of K , we placed a known concentration of malachite green G_0 and sodium hydroxide H_0 in the tank with a known quantity of salt and digitally analysed the change in the light intensity with time associated with the colour change of the fluid from green to clear. To simplify our analysis, the concentration of sodium hydroxide was two to three orders of magnitude larger than the concentration of malachite green in these calibration experiments, and so the reaction was pseudo first order. Therefore, the time-dependent concentration $G(t)$ of malachite green is given by the expression

$$\log\left(\frac{G(t)}{G_0}\right) \simeq -KH_0t. \quad (4.1)$$

For a range of saline solutions between zero and 7 %, by plotting $\log(G/G_0)$ against time, and determining the best fit to the slope of the resulting line, we calculated the dependence of the rate constant on salinity. This salinity, and hence density-dependent, rate constant could then be straightforwardly included within our code, to generate model predictions as discussed above.

We conducted seven experiments, with a range of parameters. We present the results of three characteristic experiments in this paper, with parameters given in table 1. For agreement with our calibration curves for the rate constant, the initial concentration of malachite green was always substantially less than the concentration for sodium hydroxide, and so it is at least plausible that one or other of the limiting well-mixed models (defined in (2.42) and (2.43)) will describe the experimental data well. As already noted, in all but one experiment, malachite green corresponded to species one, input by the source, and so we are able to monitor the concentration of the dye that comes into and eventually thoroughly contaminates the tank. In the other experiment (experiment C) we initially placed the dye in the tank (i.e. as species two) and we monitored its concentration until it eventually was completely vented out and consumed by the reaction.

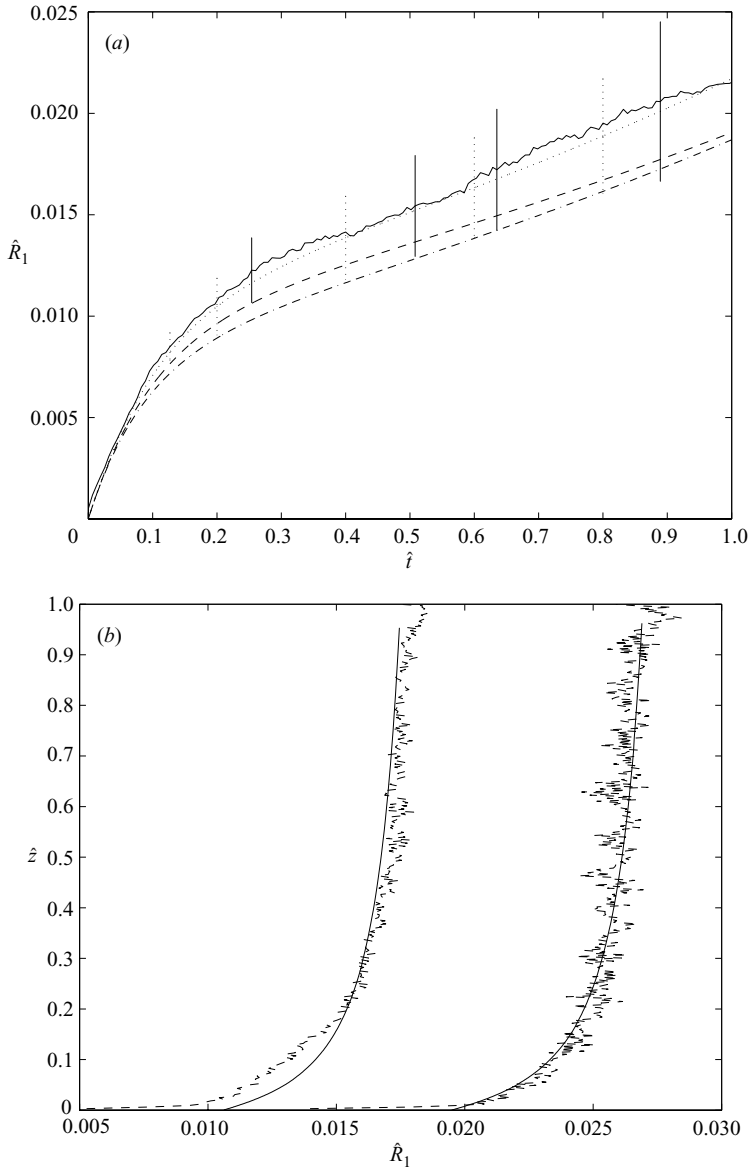


FIGURE 7. (a) Vertically averaged and (b) height-dependent plots of species one for experiment A (solid jagged line) and the plume model (dotted line on (a) and solid line on (b)), as defined in §3. The two profiles on (b) represent $\hat{t} = 0.59$ and $\hat{t} = 1.24$. The vertical lines on (a) are error bars for the numerical solution (dotted line) and experiment (solid line). We also plot the predicted concentration for species one from the well-mixed model (2.41) (dashed line) and the reduced model (2.43) (dot-dashed line) in (a). The parameters are given in table 1.

4.2. Experimental results and discussion

We have plotted the results from both the experiment and numerical method in figures 7–9. We have used $\alpha = 0.1$, a common value used in experiments. Small variations of this parameter have a negligible effect on our results. We have also assumed that the velocity was constant at the source so that given some source flow rate the source

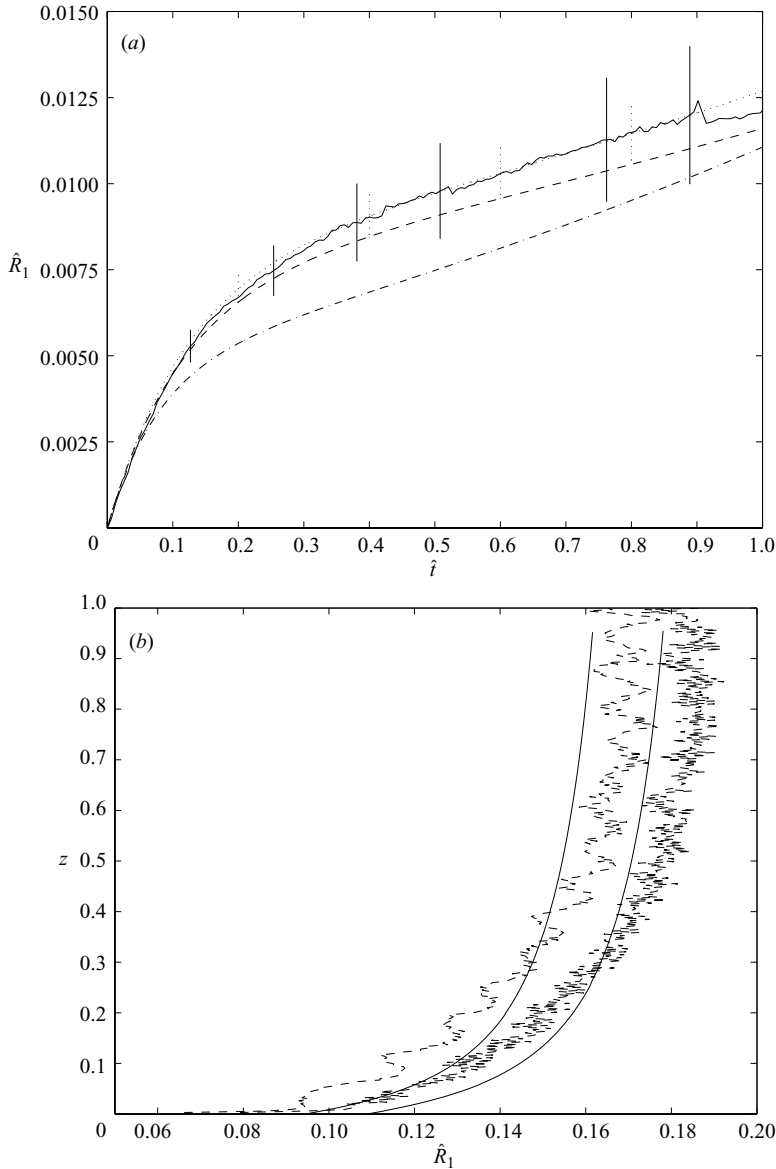


FIGURE 8. As figure 7 but for experiment *B*. The two profiles on (b) represent $\hat{t} = 0.59$ and $\hat{t} = 0.68$.

momentum flux could be determined by $M_s = Q_s^2/A_s$. In figures 7 and 8 we first plot the vertically averaged concentration of species one in the room, i.e. \hat{R}_1 , as a function of time, and then two height-dependent concentration profiles at different times. In figure 9, we plot the same quantities for species two. In all cases, we compare the experimental measurements with numerical solutions using the full model discussed in §3.

In all cases $\hat{z}_e \ll 1$, giving us a large fluid entrainment and a subsequent fast downward ambient layer velocity. Because of this, the time it takes for the first front to reach the vent in the figures shown is $\hat{t}_a = 0.075 \ll 1$. It should be noted that in

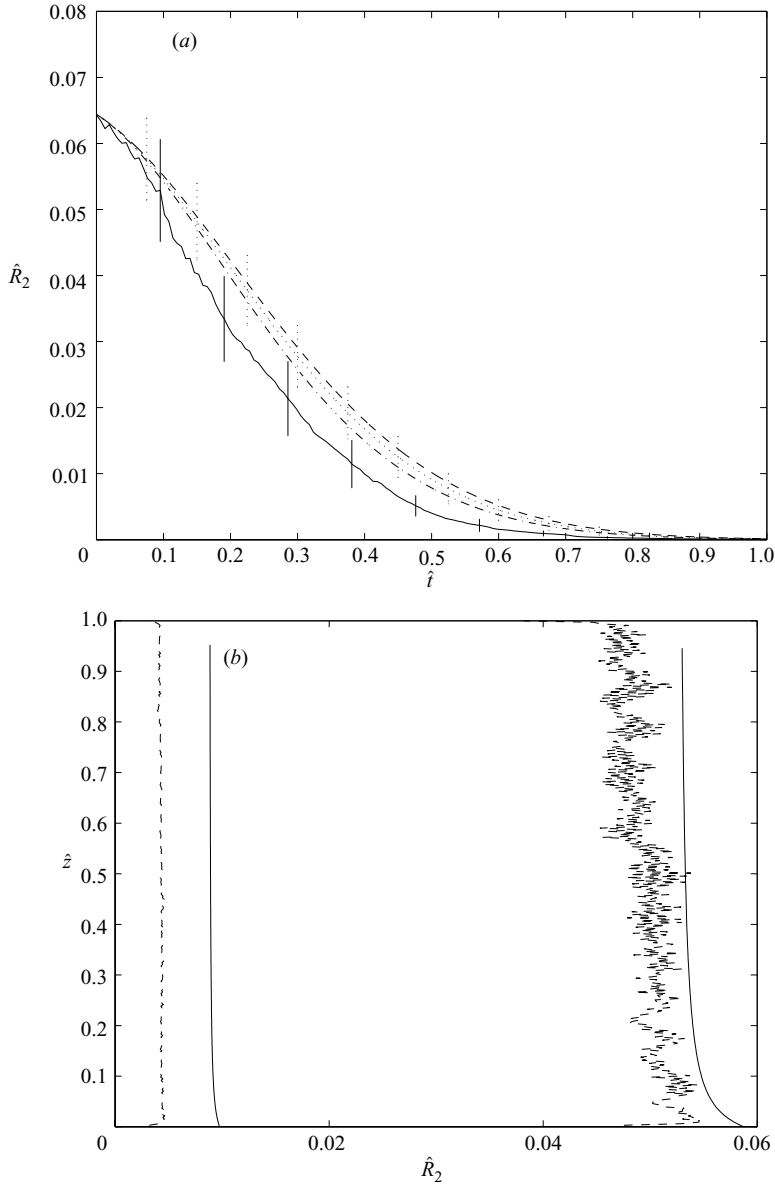


FIGURE 9. As figure 7 but for species two for experiment C. The two profiles on the bottom plot represent $\hat{t} = 0.50$ and $\hat{t} = 0.11$. The dashed line in (a) represents the well-mixed model (2.41) and the dot-dashed line represents the reduced model (2.42).

all cases the initial concentration of sodium hydroxide is about two hundred times larger than that of the dye, leading to extreme values for ϕ , for consistency with our calibration. Therefore in a region of fluid containing this large imbalance in chemical concentration, the rate of change of the base will be much slower than dye, and the reaction is pseudo-first-order. Indeed, since it can be established for the experiments shown in figures 7 and 8 that $\lambda/\phi \ll 1$, we also compare the average room concentration of species one with \hat{W}_{1b} from the well-mixed solution (2.43), while for the experiment shown in figure 9, $\lambda\phi \ll 1$, and so we compare with \hat{W}_{2a} as defined in

(2.42). In addition we have plotted the numerical solution to the well-mixed models from equations (2.41). In all cases the rate constant in the well-mixed models is a function of fluid density for consistency with the experimental results.

The error bars shown in the averaged concentration profiles are due to the uncertainty in the laboratory equipment used, such as the scale, beakers and flow meter, all of which were taken from the manufacturer's listed data. The error comes into effect in the experimental results mainly through the colour intensity–concentration calibration data and in the numerical method via the non-dimensional constants and the correction to the rate constant for density variations. It should be noted that the error bars shown in the average concentration profiles also apply to the height-dependent profiles even though they are not indicated in those figures. In all of the figures shown there is good agreement between the numerical and experimental data; the curves lie within the range of experimental uncertainty. The fluctuation in the concentration for the experiment, seen by the jagged appearance, is a consequence of the optical method used and the mean profile contains all the important physical information.

As noted above, the most obvious point of difference between the well-mixed models and both the experimental and full numerical data is during the initial stage of flow evolution, before the time \hat{t}_a when the first front arrives at the opening and contaminated fluid starts to be vented through the opening. Although this time is early in the overall flow evolution, the early behaviour has a lasting effect, and so it is clearly necessary to model the plume dynamics. The plume model sets up a concentration gradient of \hat{R}_2 (the concentration of the chemical species initially in the room) which decreases with height, where the oldest and most concentrated layer is at the bottom $\hat{z} = 0$. As a result a larger quantity of species two leaves the room sooner than if the space were well mixed, while conversely a smaller quantity of species one leaves the room, thus leading to a higher concentration of \hat{R}_1 at any particular instant compared to the well-mixed model. This result can be seen clearly in figures 7–9. (As an aside, it is necessary to allow the rate constant to increase as the density, and hence the concentration of salt, within the room decreases. This of course can be embedded straightforwardly in the numerical model, as noted above.) Overall there is good agreement between the numerical and experimental results for the plume, and in particular it is important to stress that, particularly for species one, the full plume model predicts the experimental results more accurately than the well-mixed models in a quantifiable way. In all cases, there is also a measurable vertical profile in concentration, whose amplitude decreases with time (consistently with the results of CW02 for density).

There are three distinct regions in figures 7 and 8 with different slopes that need further discussion. Before the arrival of the first front (at $\hat{t}_a = 0.075$) the concentration in the room of species one (i.e. the species entering through the plume) increases rapidly, as the only sink of this species is due to reaction with species two initially within the room. However, subsequently to the arrival of the first front at $z = 0$, fluid containing species one starts to be vented from the opening. Therefore there is another sink of species one, and so the rate of increase of \hat{R}_1 drops somewhat. This drop in the rate of increase is also related to the fact that the reaction rate increases due to a drop in the ionic strength of the fluid within the room, as salty water is replaced by the fresh water from the source. Eventually however, all the (finite quantity of) species two fluid initially in the room must be lost, due to both reaction and outflow through the vent. Therefore, the fluid within the room will approach the composition of the source fluid.

The situation is different for the evolution of species two however, as shown in figure 9. From the first instant of the experiment, since species two is initially present at all heights in the room, species two fluid is both vented from the room, and lost through reaction. Therefore, there is no markedly different behaviour for species two before the arrival of the first front. At later times, as all of species two is lost to reaction and venting, the rate of decrease drops, in a largely exponential fashion. This clearly demonstrates the approach of the system to its final steady state, with the room being completely filled with source fluid.

5. Conclusions

In this paper we have considered the theoretical, numerical and experimental aspects of a chemical reaction in an enclosed ventilated space where the flow is driven by a turbulent buoyant plume. We restricted our study to flows in which there is no diffusion between adjacent ambient layers and negligible density change from reaction. We have determined that the dynamics of this model flow can be described by five non-dimensional parameters: θ ; \hat{z}_e ; \hat{M}_s ; λ ; and ϕ (as defined in (2.7), (2.24), (2.26), (2.31), and (2.32) respectively). These parameters describe the room aspect ratio, the source volume flux, the source (specific) momentum flux, the chemical reaction rate, and the relative concentrations of the species initially in the source fluid and the room fluid. As a result of a quasi-steady-state approximation essential to the model, we are restricted to a class of problems such that $\lambda \ll \theta/\hat{z}_e^{5/3}$. To generalize the previous work of CW02, we restricted ourselves to consideration of flows where the plume entrained significant amounts of fluid as it rose from the floor to the ceiling, and so we required $\hat{z}_e \ll 1$. Unsurprisingly, as observed by CW02, well-mixed models described the evolution of the vertically averaged concentration in the room well. Nevertheless, there were measurable and observable discrepancies, principally associated with the behaviour of the system before the arrival of the first front of fluid which has been cycled through the plume.

As is apparent from the well-mixed models, the natural time scale for the fluid flow to approach its final steady state is the fluid replacement time scale t_r defined by (2.27). This illustrates the critical importance in general of the source volume flux Q_s in determining the transient behaviour of the chemical species. Typically, on this time scale, species two (the species initially in the room) is depleted through both reaction and outflow through the vent, while species one (input through the source) completely fills the room.

However, it is important to stress that this generic picture does not apply when the reaction rate is relatively large, i.e. $\lambda \gg 1$. In this case, if ϕ (as defined in (2.31)) is small, and hence the initial concentration of species two is relatively low in the room compared to the input concentration $1/\phi$ of species one in the source, species two is rapidly depleted if λ is large, on a time scale short in comparison to the fluid replacement time. Conversely, if ϕ is very large, and so the initial concentration of species two within the room is significantly larger than the source concentration of species one, the rate of increase of species one in the room is relatively slow. This is because what little species one is entering the room is being significantly depleted by rapid reaction. This leads to high transient concentrations of the product species three, and a delayed approach to the final steady state, showing that rapid reactions can dominate the fluid-dynamical filling box process for either the species entering through the source, or the species initially in the room.

Within the room, we found that the largest concentrations of the reaction product were associated with larger values of the non-dimensional reaction rate λ . This occurs because more reaction is able to occur before species two is depleted too much due to the inevitable outflow through the vent due to the input of fluid at the source. Naturally, the maximum concentration of the product species is limited by the smaller of the peak concentrations of the reacting species, as the creation of product relies inherently on the presence of both reacting species.

All chemical species were observed to exhibit non-trivial vertical profiles at finite times. Species one had a vertical structure similar to the density distribution, with higher concentrations near the ceiling of the room, associated with newer fluid layers which have been more recently cycled through the plume. On the other hand, the concentration of species two decreased with height within the room, as newer fluid layers higher in the room contained more and more fluid from the source, and less and less of the species-two-rich fluid initially in the room. Both types of profile are observed for the product species three, which at early times has profiles similar in character to species one (the species initially in the plume) while at later times, as its concentration drops towards zero, it exhibits vertical profiles reminiscent of those of species two (the species initially in the room). In all cases, the magnitude of the gradient was largest in the vicinity of the source, and decreased towards zero with time as the flow approached its steady state.

These observations have significant implications for assessment of the time-dependent behaviour of chemically reacting species within an enclosed, ventilated space. It is clear that modelling the plume dynamics using the MTT56 model improves the quality of the prediction of the evolution of the various chemical species. In particular, the early time dynamics are critical for understanding the evolution of the various species. The filling box process leads to both the development of vertical variation in concentration, but also, perhaps more importantly, a time lag before the input species is vented from the opening which inevitably leads to a mismatch between the actual flow dynamics and the behaviour predicted by well-mixed models. Even when this time lag is relatively short in terms of the time scale of the overall flow evolution towards steady state, it still leads to an observable effect on the concentration distribution within the room of the various chemical species for a significant period of time.

Now that the importance of the filling box process has been demonstrated for the evolution of chemically reacting species in an enclosed ventilated space, there are at least three straightforward yet relevant generalizations which should be considered. First, the particular location of the vent to the exterior considered in this paper is very specific. It is of undoubted interest to generalize both the location and number of the vents considered. In particular, if there are two vents at different heights within the room, there is the possibility of both 'blocked' ventilation, where the room ultimately fills with source fluid analogously to the situation described here, and also 'natural' ventilation where a two-layer density distribution develops (see Woods *et al.* 2003 for a detailed discussion, generalizing to non-zero source volume fluxes the seminal study of Linden, Lane-Serff & Smeed 1990). The evolution of the chemical species in such a layered flow would obviously be of interest.

Secondly, the particular distribution of the chemically reacting species considered in this paper, though plausible, is clearly quite special. Another highly relevant situation would be where two plumes, each of which contains a different chemical species, issue into an enclosed ventilated space. Reaction would then ensue through the mutual entrainment of fluid which has been cycled through each plume, leading to a reactive

mixture of the two different species. In the absence of chemical reaction, Cooper & Linden (1996) demonstrated that such flows lead to a complex, layered final steady state, yet the transient dynamics associated with finite source volume fluxes is an open important question.

Finally, and perhaps most significantly, the initial simplifying assumption that the chemical reaction has no dynamic role is certainly not valid in many circumstances. If the reaction is exothermic, and hence a significant amount of heat is released, the plume buoyancy flux will be increased, while conversely if the reaction is non-trivially endothermic, the plume buoyancy flux will be decreased. Such dynamic effects will modify the filling box process in a complex manner, which is undoubtedly worthy of study. For example, an endothermic reaction may actually lead to the plume fluid being dense compared to its surroundings, thus leading to deceleration of the plume fluid, and potentially collapse back towards the neutral buoyancy height for the plume fluid (see Woods & Caulfield 1992 and Caulfield & Woods 1995 for discussion of the behaviour of such reversing buoyancy plumes). Such collapse modifies qualitatively the evolution of the ambient fluid distribution, as it is necessary to model another entrainment process associated with this fluid collapse (see, for example Cardoso & Woods 1993). Furthermore, exothermic or endothermic reactions within the room fluid itself may lead to convective overturnings in the room, hence driving mixing in another non-trivial and different manner. To gain a full understanding of the evolution of chemically reacting plumes in an enclosed environment it is necessary to consider such issues, and we will report the results of our investigations in due course.

Preliminary versions of the numerical code used in §2 were developed by Adrian McBurnie at the University of Bristol and Thomas Vilmin at the University of California, San Diego.

REFERENCES

- ABRAMOVICH, M. & STEGUN, I. A. 1965 *Handbook of Mathematical Functions*, 3rd Edn. Dover.
- BAINES, W. D. & TURNER, J. S. 1969 Turbulent buoyant convection from a source in a confined region. *J. Fluid Mech.* **37**, 51–80 (referred to herein as BT69).
- CARDOSO, S. S. S. & WOODS, A. W. 1993 Mixing by a turbulent plume in a confined stratified region. *J. Fluid Mech.* **250**, 277–305.
- CAULFIELD, C.-C. P. & WOODS, A. W. 1995 Plumes with nonmonotonic mixing behaviour. *Geophys. Astrophys. Fluid Dyn.* **79**, 173–199.
- CAULFIELD, C. P. & WOODS, A. W. 2002 The mixing in a room by a localized finite-mass-flux source of buoyancy. *J. Fluid Mech.* **471**, 33–50 (referred to herein as CW02).
- COOPER, P. & LINDEN, P. F. 1996 Natural ventilation of an enclosure containing two buoyancy sources. *J. Fluid Mech.* **311**, 153–176.
- DALZIEL, S. B. 1993 Rayleigh–Taylor instability: experiments with image analysis. *Dyn. Atmos. Oceans* **20**, 127–153.
- GERMELES, A. E. 1975 Forced plumes and mixing of liquids in tanks. *J. Fluid Mech.* **71**, 601–623.
- HUNT, G. R., COOPER, P. & LINDEN, P. F. 2001 Thermal stratification produced by plumes and jets in enclosed spaces. *Building Environ.* **36**, 871–882.
- HUNT, G. R. & KAYE, N. G. 2001 Virtual origin correction for lazy turbulent plumes. *J. Fluid Mech.* **435**, 377–396.
- HUNT, G. R. & LINDEN, P. F. 2001 Steady-state flows in an enclosure ventilated by buoyancy forces assisted by wind. *J. Fluid Mech.* **426**, 355–386.
- LEVINE, I. N. 2002 *Physical Chemistry*, 5th Edn. McGraw-Hill.
- LINDEN, P. F., LANE-SERFF, G. F. & SMEED, D. A. 1990 Emptying filling boxes: the fluid mechanics of natural ventilation. *J. Fluid Mech.* **212**, 309–335.

- MORTON, B. R., TAYLOR, G. I. & TURNER, J. S. 1956 Turbulent gravitational convection from maintained and instantaneous sources. *Proc. R. Soc. Lond. A* **234**, 1–23 (referred to herein as MTT56).
- TUNNICLIFFE, V. 1992 Hydrothermal-vent communities of the deep sea. *Am. Sci.* **80**, 336–349.
- WOODS, A. W. & CAULFIELD, C.-C. P. 1992 A laboratory study of explosive volcanic reaction. *J. Geophys. Res.* **97**, 6699–6712.
- WOODS, A. W., CAULFIELD, C. P. & PHILLIPS, J. C. 2003 Blocked natural ventilation: the effect of source mass flux. *J. Fluid Mech.* **495**, 119–133.
- WORSTER, M. G. & HUPPERT, H. E. 1993 Time-dependent density profiles in a filling box. *J. Fluid Mech.* **132**, 457–466.